November 2015
Volume 121
Issue 1955
£5.20

www.electronicsworld.co.uk

Electronics WORLD

THE ESSENTIAL ELECTRONICS ENGINEERING MAGAZINE

SPECIAL REPORT

- Motor Control
- 3D-MIDs
- ROHS

Battery Stack Management
Makes Another Leap Forward

Technology
Quantum dot technology will lead to new type lighting

T&M Supplement
T&M equipment and how to buy or rent

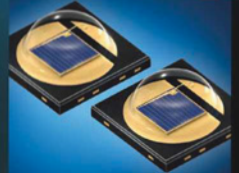

Products
EMC protective solutions, RFI shielding, certification and accreditation

IMMEDIATE SHIPMENT FROM THE WORLD'S LARGEST SELECTION OF ELECTRONIC COMPONENTS™

OPEN ACCOUNTS AVAILABLE
FOR QUALIFYING CUSTOMERS

LIVE WEB CHAT
24/7, 365 DAYS PER YEAR

FREE SHIPPING ON ORDERS OVER £50*

PRICES ARE IN BRITISH POUND STERLING AND INCLUDE DUTIES

LOCAL SALES & TECHNICAL SUPPORT AVAILABLE

Digi-Key® ELECTRONICS

0800 587 0991 • 0800 904 7786

DIGIKEY.CO.UK

1,100,000+ PRODUCTS IN STOCK | 650+ INDUSTRY-LEADING SUPPLIERS | 3.9 MILLION PARTS ONLINE

*A shipping charge of £12.00 will be billed on all orders of less than £50.00. All orders are shipped via UPS for delivery within 1-3 days (dependent on final destination). No handling fees. All prices are in British pound sterling and include duties. If excessive weight or unique circumstances require deviation from this charge, customers will be contacted prior to shipping order. Digi-Key is an authorized distributor for all supplier partners. New product added daily.

Cover supplied by
LINEAR TECHNOLOGY
More on pages 14-15

REGULARS

TEST & MEASUREMENT SECTION

T&M Supplement Cover supplied by
TELEDYNE LECROY
More on pages 48-49

FEATURES

EDITOR: Svetlana Josifovska
Tel: +44 (0)1732 883392
Email: svetlanaj@sjpbusinessmedia.com

SALES: James Corner
Tel: +44 (0)20 7933 8999
Email: jamesc@electronicsworld.co.uk

Philip Woolley
Tel: +44 (0)20 7933 8989
Email: philipw@sjpbusinessmedia.com

DESIGN: Tania King

PUBLISHER: Justyn Gidley
ISSN: 1365-4675

PRINTER: Buxton Press Ltd

SUBSCRIPTIONS:
Subscription rates:
1 year: £62 (UK);
£89 (worldwide)
Tel/Fax +44 (0)1635 879361/868594
Email: electronicsworld@circdata.com

SJP business media
2nd Floor,
52-54 Gracechurch Street,
London, EC3V 0EH

Follow us on Twitter @electrowo

Join us on LinkedIn

10 PORT & 20 PORT USB CHARGING & SYNC HUBS

Powersolve professional USB charging & sync hubs are ideal for schools, businesses or in fact any application requiring multiple connection to USB devices, for either charging or data transfer

PSUSB-10CH & PSUSB-20CH

Features

- Charges and syncs up to 10 devices (PSUSB-10CH), or 20 devices (PSUSB-20CH)
- Charge current 2A for 10 port hub and 1.1A for 20 port hub
- Supports high speed 480 Mbps, full speed 12 Mbps and low speed 1.5 Mbps operation
- Compatible with all USB compliant devices
- 10 or 20 USB 2.0 downstream ports, depending on model
- Over current detection and protection and surge and ESD protection
- 3 x 10 port devices can be connected in cascade to give up to an optimum of 30 USB ports
- 2 x 20 port devices can be connected in cascade to give up to an optimum of 40 USB ports
- Supports Windows 98SE/ME/2000/XP/Vista/7/8/ and Mac OS 8.6/9.X/10.X and higher

10 Ports 60 & 120 Watts USB Charger (charging only)

PLV120-USB

Features

- Universal 90-264VAC Input
- IEC320 C8 2 pin AC Input Connector (UK power cord included)
- Output ports, 10 x 5V 2.4A
- Will charge any device powered by standard USB charging technology, with smart charging IC
- EMC to EN55022'B', CISPR22 'B' & FCC 'B'
- Full International Safety Approvals & CE marked
- Compact Desk Top Enclosure with On/Off switch
- Meets ROHS requirements

Features

- Universal 90-264VAC Input
- IEC320 C8 2 pin AC Input Connector (UK power cord included)
- Outputs switchable from 10 x 5V 1A or 5 x 5V 2.4A
- Will charge most devices powered by standard USB 5VDC chargers
- EMC to EN55022'B', CISPR22 'B' & FCC 'B'
- Full International Safety Approvals & CE marked
- Compact Desk Top Enclosure
- Meets ROHS requirements

PLV60-USB

POWER SOLVE

www.powersolve.co.uk

Tel: 44-1635-521858 Email: sales@powersolve.co.uk

MICROCONTROLLER MARKET GROWTH TIED TO RISE IN THE INTERNET OF THINGS

The market for microcontroller units (MCUs) used in Internet of Things (IoT) applications is on the rise, bouying up the overall MCU market growth.

The number of MCUs used in connected cars, wearable electronics, building automation and other IoT applications is expected to grow, with a compound annual growth rate (CAGR) of 11%, from $1.7bn in 2014 to $2.8bn in 2019, while the overall MCU market grows at a CAGR of 4% during the same timeframe, says analyst house IHS.

"While some still consider it hype, the IoT trend has already begun disrupting the MCU market," said Tom Hackenberg, senior analyst at IHS Technology. "In fact, without the influence of IoT application growth, the MCU market is predicted to stagnate by the end of the decade."

According to the latest *Microcontroller Market Tracker* from IHS Technology, IoT comprises both existing Internet Protocol (IP) addressable devices and Internet-connectable electronic devices. This definition differs from the Internet of Everything (IoE), whereby even unconnected electronics and unconnected objects are expected to be represented on the web.

IHS divides the IoT market into three distinct categories: controllers (PCs and smartphones), infrastructure (routers and servers) and nodes (CCTV cameras, traffic lights and appliances).

"Each of these categories offers a distinct opportunity for suppliers of hardware, software and services," said Hackenberg. "The IoT trend has a strong relationship with the MCU market, as the small nodes used for connectivity and sensor hubs to collect and log data are primarily based on MCU platforms. Most serious suppliers of MCUs are already closely following this trend around the billions of connected devices; however, the industry's challenge now is to quantify this new opportunity, since IoT is a conceptual trend, not a device, application or even a new feature."

Given that IoT connectivity demands a new consideration of semiconductor features, many semiconductor companies have started developing IoT platform solutions, while others have created IoT divisions to address this opportunity. This is especially true in the MCU market.

Among the semiconductor suppliers adopting IoT-focused strategies are Atmel, Broadcom, Cisco Systems, Freescale Semiconductor, Infineon Technologies, Intel, Microchip Technologies, NXP, Qualcomm, Renesas Electronics and Texas Instruments.

"IoT is a sweeping term that addresses broad opportunities for hardware, software and services across many different applications," said Hackenberg. "Suppliers must therefore focus on their target markets and concentrate on the specific values they bring to these markets."

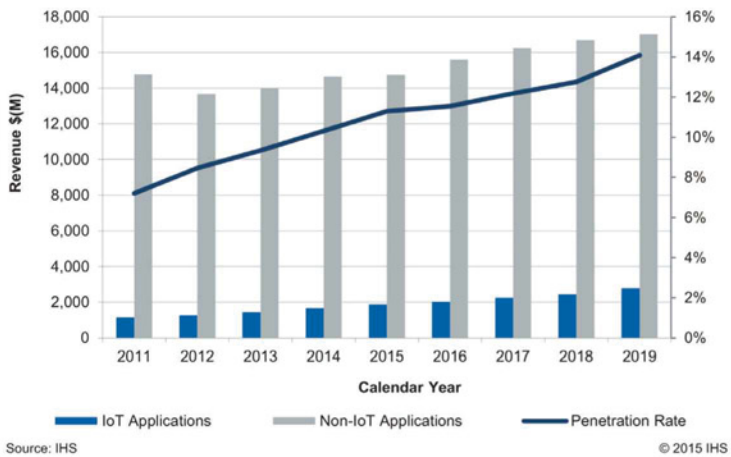

MCU market in IoT applications compared to markets outside of IoT

IHS is provides industry insight, analytics and expertise. Headquartered in Englewood, Colorado, in the US, IHS can be reached online at www.ihs.com

QUANTUM DOT TECHNOLOGY WILL LEAD TO PREFERRED LIGHTING

Advances at Oregon State University in manufacturing technology for quantum dots may soon lead to a new generation of LED lighting that produces a more user-friendly white light, while using less toxic materials and low-cost manufacturing processes based on microwave heating.

The cost, environmental and performance improvements could finally produce solid state lighting systems that consumers really like and help cut lighting bills almost in half, compared to incandescent and fluorescent lighting, according to research.

The same technology might also be widely incorporated into improved lighting displays for computer screens, smartphones, televisions and other systems.

"There are a variety of products and technologies that quantum dots can be applied to, but for mass consumer use possibly the most important is improved LED lighting," said Greg Herman, associate professor at the OSU College of Engineering.

Key to the advance is the use of both a "continuous flow" chemical reactor and microwave heating technology conceptually similar to the ovens found in the modern kitchen.

The continuous flow system is fast, cheap and energy-efficient; while microwave heating helps with the precise control of heat needed during the process. The microwave approach will enable development of nanoparticles of exactly the right size, shape and composition.

QUANTUM DOTS

Quantum dots are nanoparticles that emit light, and by precisely controlling their size, the colour of the light can be controlled.

Although they've been in use for some time, they are expensive and lack optimal colour control. However, organizations such as OSU are developing manufacturing techniques for scaling up to large volumes for low-cost commercial applications, and provide new ways to offer the precision needed for better colour control.

"Taggants" – compounds with specific infrared or visible light emissions, are used for precise and instant identification, including control of counterfeit bills or consumer products.

APPRENTICESHIP SCHEME RECEIVES UNPRECEDENTED 7,500 PLEDGES IN JUST FOUR MONTHS

QA Apprenticeships's 10KinTech initiative has passed the 7,500 mark since its launch in June this year. The scheme was set up to help fill the technology skills gap in the UK, and last year it placed some 5,000 new apprentices in jobs in the IT and technology sectors. The goal is to place another 5,000 by the summer of 2016, part of a bigger scheme that supports the Government's plan to create 3 million apprenticeships across the UK by 2020.

"It's really encouraging to see what QA is achieving through 10KinTech. I've been so impressed by the quality of apprentices I've met: confident, articulate young people who are enthusiastic, highly committed and excited about their prospects," said Maggie Philbin, CEO of TeenTech CIC. "We all know there is a huge demand for young people with the right skills for contemporary industry, but not enough parents and teachers realise that a high-quality IT apprenticeship is an extremely valuable career route."

Maggie Philbin is CEO of TeenTech CIC and a well-known UK TV personality

The scheme has support from blue-chip companies, including HP and Microsoft. "[At] Microsoft [we] look forward to welcoming more QA apprentices into the business this year as part of our commitment to 10KinTech," said Jacqui Lloyd, Early in Career Programme Manager.

QA takes candidates from GCSE-level through to MSc.

NEW STANDARD FOR NON-ISOLATED DIGITAL POINT-OF-LOAD

The Architects of Modern Power (AMP Group) consortium announced a new standard last month aimed at establishing common mechanical and electrical specifications for advanced power-conversion technology in distributed power systems. The picoAMP standard, designed for the lower-power range for board-level conversion needs, provides customers with a non-isolated standards platform ranging from 6-18A. The standard defines a compact footprint of 12.2mm x 12.2mm in a land-grid-array (LGA) format.

"The picoAMP standard is the next step for the AMP Group in standardizing all areas of the digital power market," said Carlos Bustos, Vice President of Global Strategic Product Marketing at Murata Power Solutions.

The new picoAMP standard builds on the previously released teraAMP standard for non-isolated digital point-of-load (POL) DC-DC converters, released in February 2015, and the microAMP and megaAMP standards released in November 2014.

The first products to meet with the new picoAMP standard will be announced by AMP Group members by the end of 2015.

The goal of the AMP Group's alliance between CUI, Ericsson Power Modules and Murata is to realize the most technically advanced end-to-end solutions and provide a complete ecosystem, including hardware, software and support. Beyond purely mechanical specifications, it is the standardization of monitoring, control and communications functions, and the creation of common configuration files for plug-and-play interoperability that will ensure compatibility between each firm's products.

BEHIND EVERY HASSLE-FREE PURCHASE

THERE'S A DISTRIBUTOR YOU CAN COUNT ON

Our one-stop shop approach means you only need one supplier, while our competitive pricing ensures you get the best value. With no minimum order quantity available across an extensive range of electronics, automation and control, and tools and consumables, you can count on us whether you need a few parts or many.

uk.rs-online.com

RS

THIS SERIES PRESENTS THE RASPBERRY PI SINGLE-BOARD COMPUTER, ITS FEATURES AND BENEFITS, AND ITS USE IN VARIOUS PROJECTS

The Raspberry Jazz Glitter Trio

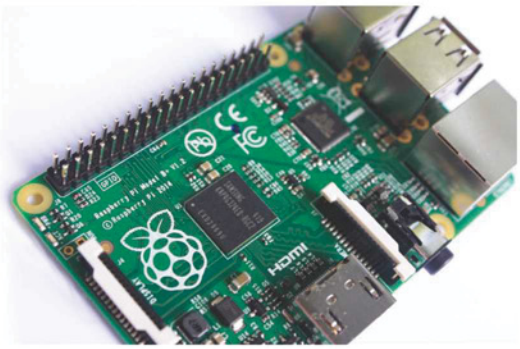

BY **MIKE COOK, JONATHAN EVANS** AND **BROCK CRAFT**

This is a fun project that creates a free jazz trio inside the Raspberry Pi.

Some people joke that free jazz got its name because no one would ever pay for it. Although jazz may be an acquired taste, this is still a fascinating little project. A webcam is pointed toward a glitter lamp (glitter floating in liquid), so the camera acts as a high-resolution multicolour sensor. This data is then gathered from the glitter lamp to trigger the sounds for the project, thus creating free jazz.

The 'Band'

Figure 1 shows our version of the Raspberry Pi jazz glitter trio. Yours may be a bit different, depending on the materials you're able to gather. There are should be two main components: a cheap webcam and a glitter lamp, which we picked up from a thrift store for less than $10.

The glitter lamp we chose was the smallest we could find; it's about 5 inches tall and contains silver glitter suspended in liquid. When the lamp is still, the glitter slowly floats up. When the lamp is turned upside down, a tilt switch in the base triggers a circuit to start one minute of random pulsing of three different coloured light-emitting diodes (LEDs), illuminating the glitter from the lamp's base. As the glitter drifts and tumbles, it catches the light from the LEDs and sparkles. Because the LEDs are in different positions, different bits of glitter get illuminated with different colours.

Both the lamp and the webcam are mounted on a box. The box includes a back shield so that only the glitter is picked up and stray light is reduced. (Construction plans for the box are included as part of the project.)

The Webcam

Webcams come in many shapes, sizes and resolutions. For this project, aim for the cheapest you can find. The resolution doesn't matter much for this project, so a low-resolution webcam will do nicely.

Here's what to look for in a webcam for this project:

- **Compatibility:** The most important thing is that the camera be supported by the Raspberry Pi's Python-based software (and most low-cost generic cameras seem to be).
- **Access to the interior of the webcam:** You need to be able to physically get into the camera so you can mount it. Look for a webcam with small screws on the outside of the case rather than an all-in-one moulded case. You're going to be hacking into the USB power lead to power the glitter lamp's LEDs.
- **Manual focus:** Make sure the webcam has a manual focus lens. Fixed-focus types are hard to adjust for very small distances, which is what you need for this project.

You can buy the webcam we used at http://uk.farnell.com/trust/17003/webcam-exis-trust-uk/dp/1860369. For a complete list of Raspberry Pi USB webcams, check out www.elinux.org/RPi_USB_Webcams.

Testing The Webcam

The first step is to test that the webcam works and is supported by the software. Create a directory for the project called 'glitter', either from the desktop or by typing the following from your home directory (or wherever you want to work):

mkdir glitter
cd glitter

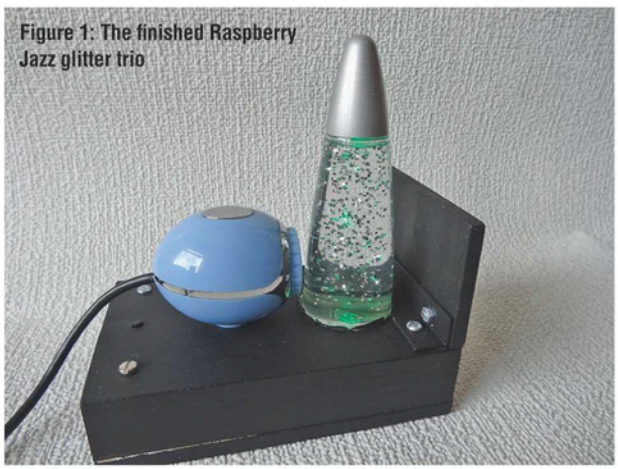

Figure 1: The finished Raspberry Jazz glitter trio

Next, download the support files you need by typing the following:

sudo wget http://www.cl.cam.ac.uk/downloads/freshers/image_processing.tar.gz

To extract the files, just type:

sudo tar -xf image_processing.tar.gz

This gives you the support software and some basic tutorial files on how to use the software; but, for the time being, ignore these and install the Python libraries. First, navigate to the libraries directory and then install the libraries by typing:

sudo cd library
sudo make install

This executes a script that moves all the files and library code into the necessary places in Python's file system. Now you're ready to try out the camera. Create a file, using the code shown in Listing 1, and store it in your glitter directory. Give it the title of 'camTest.py', plug in the webcam, change the directory of the prompt to the glitter directory, and run the file by typing the following:

python camTest.py

Listing 1: Camera test:

```
from imgproc import *
import time
my_camera = Camera(320, 240)
my_image = my_camera.grabImage()
my_view = Viewer(my_image.width, my_image.height,
"WebCam")
while True:
my_view.displayImage(my_image)
time.sleep(0.1)
my_image = my_camera.grabImage()
```

Reading step-by-step through this listing gives you an idea of what's going on. First, import the module that supports the webcam, as well as the time module. Then define an instance of the camera class and specify the size you want it to be. Here, it's only 320 x 240 pixels, so it's not very high resolution. (Later, you can make this even smaller.)

Next, the listing grabs an image from the camera's 'vision' and defines a view window for later display of this image on-screen.

Last, the program goes into an endless loop displaying the image, sleeping (or delaying) for 0.1 seconds, and then getting a new image.

The result is that you see the image from your webcam in the top-left corner of the screen. If this fails, your webcam is probably not supported by the Raspberry Pi and you'll have to get another one for the project.

If your webcam works, check that you can focus to half an inch or so; if you can't, you may be able to adjust the lens when you take the camera apart.

Hacking The Glitter Lamp

You can set up your camera to point to the glitter lamp and turn it on manually – this will give you some idea of what the finished project's sound will be like. However, by hacking the glitter lamp and the camera, you get a neat compact unit all powered by the USB connection, and you can easily invert the lamp to get the glitter all mixed up again. You may have to modify these instructions depending on how your lamp and camera are constructed.


Figure 2: Our glitter lamp

Note that at this point you may want to skip to the software section, and get the system going without doing any hardware hacking. Feel free to skip ahead and come back to this section later.

Besides a glitter lamp and a suitable webcam, the other parts we used include:

- ¼in plywood or medium-density fiberboard (MDF) to make the box – two pieces 3in x 5in and one piece 3in x 2in;
- A ¾in x 16in strip of pine for the box sides;


Figure 3: The glitter part of the lamp

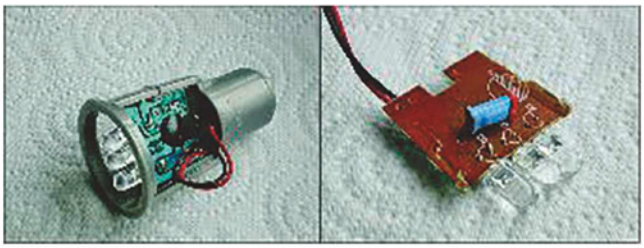

Figure 4: (left) The circuit board in the plastic assembly; (right) the shows the removed printed circuit board (PCB)

- A tack switch with ¼in plunger;
- A 3in length of 3/8in aluminum;
- Matte black paint;
- Four 18mm M3 tapped hexagonal standoffs;
- Ten 10mm pan-head M3 screws;
- Two M3 nuts;
- Wood glue, hot glue and connecting wire.

Our glitter lamp is shown in Figure 2. It is powered by three self-contained coin cell batteries. Except for the battery compartment, we could see no way into the lamp, so eventually we resorted to drastic measures and cut all around the base with a saw, leaving it looking a bit truncated, as shown in Figure 3. This left the electronics in the other half of the lamp.

In Figure 4, the photograph on the left shows the circuit board in the plastic assembly, and the photograph on the right shows the removed printed circuit board (PCB). That long component on the top is the tilt switch; it consists of a small metal ball inside a tube that makes a circuit between the two wire ends when the lamp is tilted past a certain angle. ●

RASPBERRY PI PROJECTS FOR DUMMIES

This column is an edited extract from 'Raspberry Pi Projects For Dummies' by Mike Cook, Jonathan Evans and Brock Craft, published by Wiley.

If you want a copy of the book, enter our giveaway by sending an email to the Editor at svetlanaj@sjpbusinessmedia.com, with the book's title in the subject field.

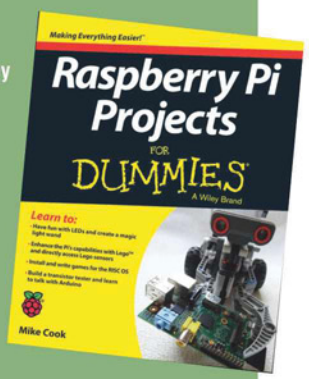

In Praise Of Simple Processors

BY **MYK DORMER**

We are living on the steep, ascending slope of Moore's Law. Complex silicon devices surround us in almost every area of commerce or industry, and become more capable and complex by the day. Any engineer with even a single grey hair will remember some far from distant time when their desktop computer's bulky and expensive hard drive was orders of magnitude smaller than the flash memory integrated into their MP3 player, or given away as a promotional USB drive at some trade show or other.

Embedded design – and its awkward cousin, low-power wireless – are not unaffected. Microcontrollers, once limited to simple four- and eight-bit devices with limited memory and scanty peripheral functions, have exploded into a huge variety of sophisticated systems, combining large amounts of storage with highly capable fast-clocking processing cores and a bewildering choice of peripheral devices.

With this increase in processing power has also come an immense increase in the range of programming tools available to firmware developers, with high-level languages (most notably, but not only, the various dialects of C), complex development environments and even whole (specifically optimised) operating systems finding their way into relatively low-end applications. With the burgeoning Internet of Things and the penetration of complex software-stack-based communication protocols (ZigBee and Wi-Fi) into the industrial telemetry area, this tendency is on the increase.

Perhaps this is why fellow engineers, when they see that my first port of call in any embedded control design is assembler code running on a very simple processor (little different from the architectures of the late 1970s), either think I am insane, a throwback or – once the job is successfully completed – a magician.

"Why don't you code that in C (or Java, or Python, or whatever) on this, or that new processor (more powerful than my desktop development machine)?", is a question I have heard more than once. So let me explain:

The increased sophistication and capability of each new generation of silicon tends to obscure the fact that the same improvements in technology, fabrication geometries and memory processes are also, at the same time, incrementally improving the very low end devices as well. Rather than adding complexity, these improvements allow a smaller die size and a higher yield, so that it is now possible to buy a very simple (but still very useful) 8-bit device in a low pin-count package for under £0.30.

Such devices still (somewhat) resemble first-generation microcontrollers in terms of architecture, and therefore are still best handled in low-level machine code, but that is the end of the resemblance. As well as being inexpensive, they are miserly in terms of power consumption, will operate at low clock rates and have very small EMI footprints.

Of course, it is always possible to execute a simple task with a complex processor, and that can (sometimes) allow a more programmer-friendly high-level language to be used (with the associated advantages of pre-written arithmetic and device driver libraries), but while less taxing for a high-level-language trained software engineer, the result will be more expensive and will frequently require more processing cycles, and hence a faster clock, more current and higher levels of RF interference.

I am not advocating the retention of earlier generation silicon here. It would be madness to design in some archaic 5-micron NMOS part with today's catalogue of devices available, but I am challenging the assumption that a more sophisticated solution to an existing simple requirement is always better. By applying processor- and memory-intensive methods of firmware design to low-end control applications I fear that we are trying to use the same (powerful) tool for every job, and not just those where such methods are undoubtedly necessary. (I am not suggesting that in 2015 anyone should have to write a web-server in assembler, or control a power station without the safety net of a sophisticated RTOS or software certification tools).

I am recommending a more graduated approach to how control problems are solved. Extremely simple or very time-critical functions are still best handled with combinatorial logic, either discrete hardware, of programmable, FPGA-type devices. Then comes a layer of simple processing, such as data coding/decoding, the lower levels of data network design, or simulation of complex state machines, where minimalist processors running a few hundred, or thousand, lines of assembler are the best fit – and only well above this level should we start looking at high-level languages and fast, complex, processing systems.

It's a matter of using the right tool for the specific job, rather than picking up a hammer and deciding that everything is a nail. ●

Myk Dormer, Consultant Engineer, Radiometrix Ltd
www.radiometrix.com

Same-Band Combining Technology Improves LTE Deployment

BY **JUAN IROLA**

The rising demand for mobile capacity is driving network operators to migrate to more spectrum-efficient technologies, the most popular of which is LTE. To add LTE without disrupting legacy 2G/3G services, many operators are choosing LTE overlays, as opposed to investing in a single radio access network (RAN) that integrates 2G, 3G and 4G services. The major advantage of an overlay approach is cutting the time-to-market. Today, as many as 75% of all LTE deployments are overlay.

Models In Use

For operators looking to deploy LTE using an overlay approach, there are two primary models currently in use. The first involves co-siting dedicated LTE RAN equipment alongside the existing infrastructure, which includes purchasing LTE radios, antennas and feeders, and erecting additional towers or poles where necessary.

This dedicated RAN model has several performance-related benefits: it provides independent control of the LTE and legacy antennas, enabling operators to optimize coverage patterns and tilt

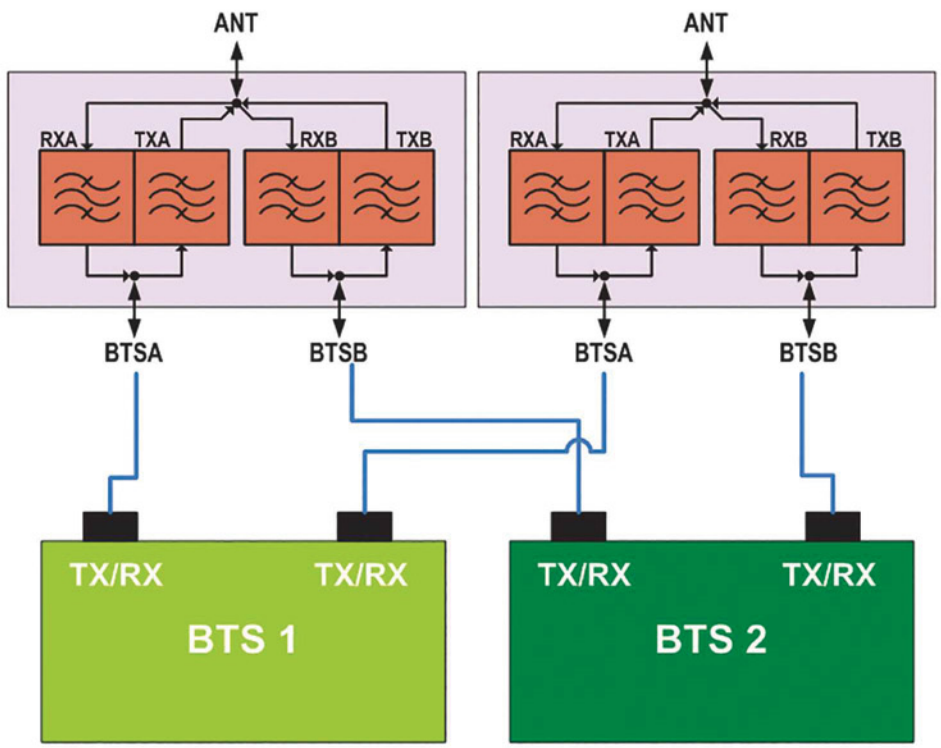

Figure 1: A 4x2 configuration for the duplex-duplex combiner can be used to support the MIMO capabilities now common in many of today's radios and antennas

settings for each service. This could also reduce concerns regarding potential interference between systems, and minimize RF path loss within both systems. In addition, this model allows operators to work on one network without affecting service on the other.

However, there are obvious obstacles to deploying a separate co-sited LTE network, the biggest of which are the added cost and time involved in bringing the new service on line. Other constraints relate to site architecture and regulatory compliance that can often reduce the system designer's options. In most situations, factors that must be considered include:

> Today, as many as 75% of all LTE deployments are overlay

- Zoning restrictions on the quantity and design of antennas and other equipment.
- Limits on weight and wind loading of feeders and tower-mounted equipment.
- Cost-savings opportunities on capital expenditures, lease costs and installation labour.

For these reasons, many operators reuse as much of their existing RF path as possible by using same-band combining. This enables use of their current feeders and antennas to support legacy 2G/3G services with the new 4G LTE service. As a result, they are able to maximize the value of existing infrastructure, reduce CapEx and accelerate the return on investment (ROI) of their LTE services.

It should be noted that in some instances antennas may need to be upgraded in order to support both LTE and legacy services; but, overall, this equipment-sharing model provides excellent balance between cost, time-to-market and quality of service.

Combiners

For operators who choose the path of antenna sharing, the signal combiner is a critical component. Same-band combiners (SBC) are RF modules designed to combine base stations with the same or different technologies in a similar frequency band with a common antenna. The combiners can be positioned at the top of the tower or the base transceiver station (BTS) at the tower base. Important performance characteristics include:

- Low insertion loss;
- Wide operational bandwidth;
- High band-to-band isolation;
- Impedance matching at all ports.

The hybrid combiner is a directional coupler in which two coupled transmission lines are set close enough together to allow energy passing through one to couple to the other. It provides a low-cost method for combining uplink and downlink signals for frequencies within the same band.

The main disadvantage to the hybrid combiner is the 3dB insertion loss in both the TX and RX signals. This can translate into a 50% reduction in output power for both LTE and legacy systems. The loss increases steeply with the number of ports combined.

Until recently, operators were somewhat limited with the available combiner technologies. Recently, a new class of same-band combiner has been introduced for use with LTE. The duplex-duplex is a 2x1 combiner that supports duplex traffic on both the uplink and downlink paths, while keeping insertion loss typically below 1dB for transmit and receive signals. This makes it compatible with all LTE radios, as well as with all 2G and 3G BTS systems. When deployed in tandem, in a 4x2 configuration (Figure 1), it can be used to support MIMO capabilities now common in many of today's radios and antennas.

Specific Designs

The duplex-duplex design was developed in response to operators' growing need to deploy LTE overlays more quickly and efficiently. The design shown in Figure 1 was engineered by CommScope in partnership with a major North American multi-network operator (MNO). The operator had allocated a limited amount of spectrum (10+10MHz) within its 1900MHz band for its LTE deployment.

Many of the markets selected for the LTE rollout had high capacity demands that couldn't be met using the hybrid combining technology. CommScope engineers worked with the operator to adapt the design shown in Figure 1 to meet the performance specifications of the selected locations.

For operators considering deploying the new combiner solution, this project highlights the importance of carefully weighing several factors in order to select the best technology. The key variables are:

- Frequencies to be combined;
- Capacity requirements;
- Budgeted insertion loss.

As capacity demand continues to skyrocket, available spectrum will become harder to come by. Spectrally-efficient technologies like LTE will be critical for satisfying demand, so too will the ability to take advantage of smaller isolated blocks of spectrum. ●

Juan Irola is principal electrical engineer at CommScope. This column is an edited extract from CommScope's new eBook, 'LTE Best Practices'. Different authors of this eBook will contribute articles to this section.

BATTERY STACK MANAGEMENT MAKES ANOTHER LEAP FORWARD

By Greg Zimmer, Senior Product Marketing Engineer, Signal Conditioning Products, Linear Technology Corp.

Any doubts about the viability of electric vehicles have long been put to rest. The primary question now is "how far, how wide and how deep will this new high-power battery technology penetrate?" Perhaps not surprisingly, no one really knows for sure. But it is interesting to consider the evolution of the battery management system (BMS) electronics, and specifically the multicell battery monitor electronics at its heart. Doing so may provide clues to the adoption rate of high voltage battery packs in applications ranging from battery backup systems to exoskeletons. Let's consider the advances made in one family of products, Linear Technology's LTC68xx, in terms of safety, accuracy, functionality and development tool support.

In 2008, Linear Technology announced the first high performance multicell battery monitor, the LTC6802. Among its key features, this part included the ability to measure up to 12 Li-Ion cells with 0.25% maximum total measurement error within 13ms. The key capability of these multicell battery monitors is that many can be connected in series, enabling synchronized monitoring of every cell in very long, high voltage battery strings (Figure 1). Since that time, Linear Technology has followed up with the LTC6803, LTC6804 and now, its most advanced multicell battery monitor, the LTC6811. All four of these parts serve the same basic function: they measure the voltage on each battery cell of 12 series-connected cells. The evolution of this family tracks continuous improvements in functional safety, measurement accuracy and integrated functionality.

The most dramatic progress of the battery monitor electronics is the development of functional safety, as defined by the ISO 26262 standard. In essence, ISO 26262 systematically addresses potential hazards in an automobile that could be caused by the malfunctioning behavior of electronic and electrical systems. Although the ISO 26262 standard involves nearly every phase of product development and use, the system designer must focus on how to continuously confirm the proper operation of every element that could impact safety. The multicell battery monitor plays a central role in this task, since incorrect voltages on the battery cells are the first indicators of a potential problem. This presents a significant design challenge.

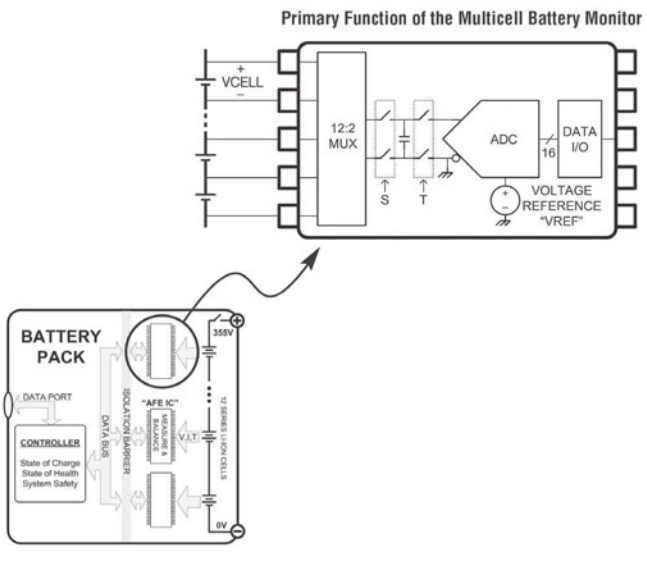

Figure 1. Simplified Description of the Multicell Battery Monitor

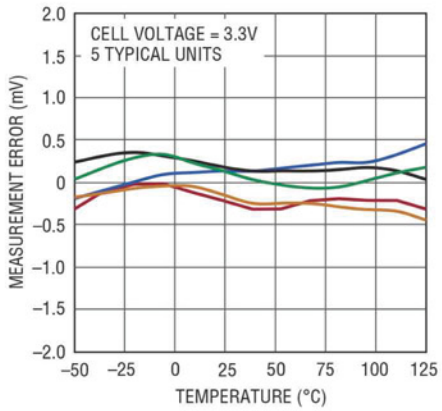

Figure 2. Outstanding Temperature Drift Performance of the Buried Zener Voltage Reference

Built into the DNA of Linear Technology is the determination to pursue tough analog electronic problems, and automotive electronics are no exception. The multicell battery monitors illustrate the achievement of high reliability, high stability, and high measurement accuracy, with the expectation of years of operation in an environment of high voltages, extreme temperatures, hot plugging and electrical noise. The ISO 26262 standard goes one step further by requiring, among other things, an analysis of potential failures and their remedies. A common method within electronics to recognize and remedy potential failures is to include self-test capability and redundancy. Even before the publication of the ISO 26262, Linear Technology recognized the importance of functional safety and included self-test capability and internal redundancy in the LTC6802. Each new generation of multicell battery monitors added and refined this capability. The latest device, the LTC6811, continues this progression, with improvements to increase its internal diagnostic coverage. These functions include additional redundant measurement paths, improved synchronization between input signals, and improved self-test accuracy. The result is quicker, simpler and more efficient self-tests to help designers achieve their ISO 26262 goals. Even for non-automotive applications, these

features give the designer confidence for whatever high reliability applications that they target.

The Linear Technology parts have steadily improved and innovated in cell measurement accuracy. Pursuing outstanding accuracy has always been a key design goal because potential measurement error translates to less effective battery management, and ultimately less pack capacity, reliability and/or life. Significant effort was made to optimize the built-in voltage reference, since it is the primary determinant of measurement error. The first Linear Technology multicell battery monitors incorporated a bandgap voltage reference. This was the conventional choice, since bandgap references are small, low power and low dropout. However, a bandgap reference can behave like a strain gauge, converting mechanical stress from PCB assembly, thermal variations, humidity, and long-term drift into measurable error. To avoid this limitation, Linear initiated a unique approach by adding a dedicated sub-surface Zener voltage reference to the design. These references offer outstanding stability, over temperature, time and other operating conditions. The result, available today in the LTC6811, is the ability to measure every battery cell to worst-case accuracy of better than 1.2mV (Figure 2).

Furthermore, the Linear Technology parts ensure outstanding measurement accuracy, even in the presence of noise, by filtering the noise on each battery cell voltage. This is accomplished by using delta-sigma analog-to-digital converters rather than the fast SAR converters, commonly used in alternative approaches. Once again, Linear Technology chose to break from the pack, despite the clear speed advantage of SAR converters when measuring hundreds of individual battery cells. This choice was made because the automotive environment is chock-full of noise and transients from motors, solenoids, power inverters, etc. All of this noise affects measurement accuracy. With a delta-sigma converter, the input is sampled many times over the course of a conversion and then averaged. The result is built in low pass filtering to eliminate noise as a source of measurement error, where the cutoff frequency is established by the sample rate. For example, the LTC6802 uses a 2nd order delta-sigma that operates at a fixed 1k sample per second. The result is 36dB of rejection to 10kHz switching noise (Figure 3). The trade-off however, is that measuring 12 cells with the LTC6802 requires 13msec, which is too slow for some applications. Nonetheless, using a delta-sigma converter has remained the most practical method for achieving accurate cell measurement in the noisy real world. For this reason, Linear has continuously improved its delta-sigma approach. Today, the LTC6811 uses a much faster 3rd order delta-sigma ADC with programmable sample rates and 8 selectable cutoff frequencies. The result is outstanding noise reduction and 8 programmable measurement rates (Figure 4), enabling measurement of all 12 battery cells as fast as 290µsec.

Finally, it is interesting to note how the functionality of the multicell battery monitor has expanded. As previously mentioned, the primary task of a multicell battery monitor is to accurately measure cell voltages and communicate this information to a host processor. Furthermore, it is best that the multicell battery monitor not include internal software, as this could present a potential conflict with the system-level battery management; the task of collecting data from all of the cells and determining the

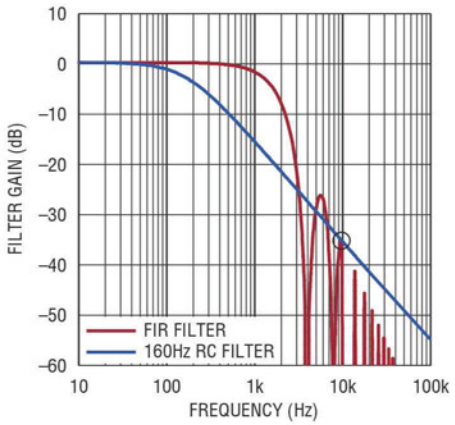

Figure 3. LTC6802 Delta-Sigma Converter vs. SAR Converter with RC Circuit.

state of charge or state of health should be accomplished by the main BMS processor. However, the multicell battery monitor resides at the most critical location in the battery system, directly connected to the cells. Here, it is in an ideal position to monitor other battery sensors, such as current or temperature, and closely correlate these values to cell measurements. For this reason, the multicell battery monitor can act as a central hub between the BMS microprocessor and peripheral devices.

Conclusions

Since 2008, Linear Technology has released four generations of multicell battery monitors. The safety features, accuracy and functionality of these devices have evolved significantly over this period, illustrating the growing importance of these ICs in high performance battery management. In addition, new tools simplify and standardize their integration into battery management systems, irrespective of the end application. Linear Technology's most advanced multicell battery monitor, the LTC6811, provides an impressive set of features for practically any high voltage, high powered battery system.

Linear Technology (UK) Ltd • Tel: 01628 477066
Email: uksales@linear.com • www.linear.com

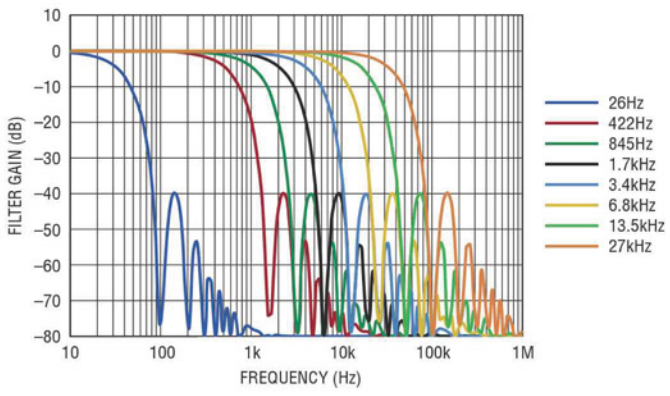

Figure 4. LTC6811 Delta Sigma Converter

LOW-POWER AND COST-EFFECTIVE SPEED CONTROL CARD FOR REMOTELY-CONTROLLED DC MOTORS

BY **DURMUS UYGUN** FROM GEDIZ UNIVERSITY IN TURKEY

There are many different methods used to meet the needs of industrial systems, for starting, stopping, monitoring, determining important conditions and implementing necessary actions. With improvements in electronics and other technologies, we are increasingly seeing industrial application control circuits that rely on remote-controlled systems, with the Internet, mobile, infrared and wireless technologies being used for communication and control.

Advantages such as ease of control and high efficiency have made direct current (DC) machines – or motors – an integral part of remote-controlled systems. Proportional-integral-derivative (PID) controllers, the control loop feedback mechanisms widely used in industrial control systems, are typically found in speed- and position-control systems. Also, digital variable speed control drivers for DC motors are easier to handle and cheaper than AC motor drivers.

Speed Control

The speed of a DC motor can be adjusted by using the following methods:

- Varying the armature circuit resistance (R_a); ("Armature" is one of the two main electrical components of a motor);
- Varying the excitation current (I_a);
- Using a Ward Leonard system (the widely-used DC-motor speed control system introduced by Harry Ward Leonard in 1891);
- Using semiconductors;
- With pulse width modulation (PWM).

The first three methods are old and their usage has gradually decreased, now mostly replaced by PWM techniques.

In PWM, the speed of a DC motor can be adjusted by changing the duty cycle of the PWM voltage, which has a constant frequency.

The duty cycle of the PWM signal (d) shown in Figure 1 is:

$$d = \frac{t_j}{t_j + t_i} \quad (1)$$

Since the armature voltage changes with the duty cycle, if a PWM signal with different duty cycle and constant frequency is applied to a DC motor, the motor's speed (ω_a) will be:

$$\omega_m = \frac{dV_a - I_a R_a}{K_m \phi} \quad (2)$$

where V_a is the armature voltage, I_a is the motor armature current, R_a is the armature resistance, K_m is the motor constant and Φ is the magnetic flux.

When the duty cycle is zero, the speed of the motor will be zero too.

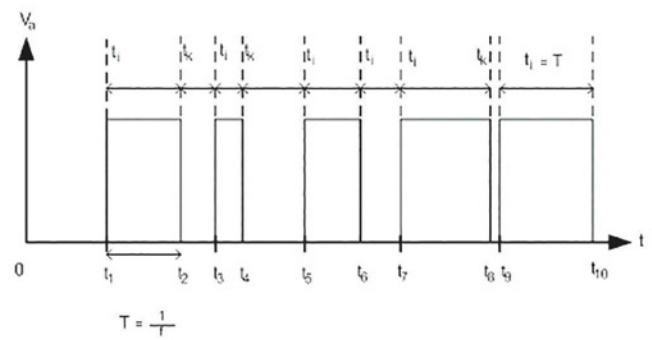

Figure 1: A PWM signal with an alternating duty cycle

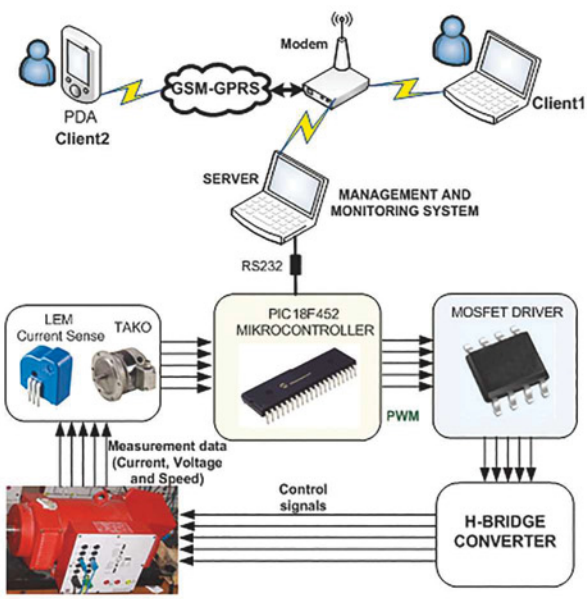

Figure 2: System flow diagram

When the duty cycle is one, maximum voltage is applied continuously and, in this case, the motor reaches its maximum speed.

The frequency of the applied PWM signal is chosen by considering the characteristics of the DC motor and the threshold frequency. Whilst in the past the optimum interval for these values was between 400-1000Hz, now the upper limit has moved to 100kHz, thanks to constant development of the DC motor drive circuits, programmable integrated circuits (ICs) and digital processors.

System Design

Figure 2 shows the functions and interactions of the components used in a real-time, Internet-monitored, control system of a DC motor.

The basic hardware list consists of:

- Supply circuit (four isolated transformer power supply circuits, 5-15V);
- Current-measuring circuit;
- Tachogenerator speed regulation circuit;
- Voltage-measuring circuit;
- Programming and control circuit (based on PIC18F452);
- MOSFET driving circuit (based on a IR2110 MOSFET);
- H-bridge control circuit (based on IRFP250 type MOSFET);
- RS232 communication protocol.

The system's power supply is handled by different channels, based on a 4-layer (5-15V) feeder circuit design, show in in box 1 of Figure 3.

Boxes 2, 3 and 4 of Figure 3 show the measurement circuit, connected to the motor shaft with the LEM current sensor, which detects the tachogenerator signals, producing 2.5V at 1000rpm. A current sensor circuit and an amplifier handle the tacho's voltage level and range; see Figure 4.

Measurements such as current, power and speed obtained during system operation can be monitored by computers via an RS232 port (box 8 in Figure 3). The computer sends commands, which are realized via a microprocessor (we used a PIC18F452, box 5 in Figure 3).

Our MOSFET drive circuit was designed with IR2110 type MOSFET drivers and optical transistors. The circuit shown as box 6 in Figure 3 processes the PWM drive signals coming from the PIC18F452 and transmits them to the IRFP250 MOSFETs to which it is connected.

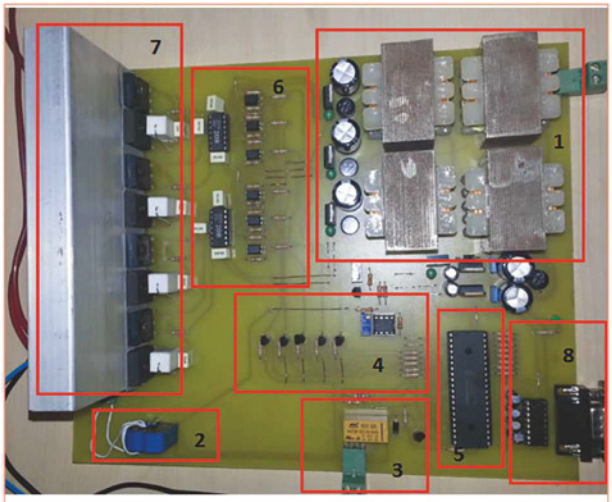

Figure 3: General view of hardware used in the system

The main reasons we chose the IR2110 driver in our application are that it takes up less space and can drive both low-side and high-side MOSFETs.

To drive the DC motor in the control circuit, our H-Bridge MOSFET converter circuit (box 7 in Figure 3) was developed with IRFP250 MOSFET (the motor feed voltage must be reversed to change the rotation direction).

Software Design

Three different interface designs were developed with the Visual Studio software program to monitor the data obtained during system operation and perform tasks such as sending data to the microprocessor when necessary. These are server software, client software and mobile (PDA) client software. The PDA uses packet switched radio services and the monitoring system is written in C#.

We tested each one, with the hardware setup (Figures 5 and 6) consisting of:

- Two shunt DC motors (one was used as a generator);

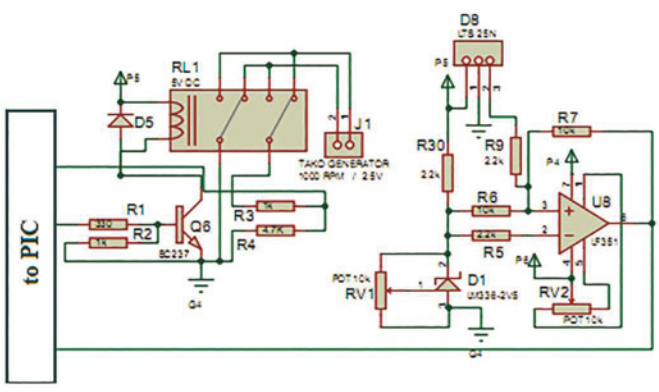

Figure 4: Tachometer circuit

Figure 5: Test setup

Figure 6: Server and client laptops, and client mobile phone used in the setup

- One tachogenerator (supplying 2.5V at 1000rpm);
- One external power supply;
- One CISCO wireless modem;
- Load group;
- Two measurement devices (for current and voltage).

We tested the software in two steps:

- First, the PWM rate was held at a constant value (80%) and the motor was loaded to nominal load. Current, power, speed and torque graphs of the motor at the server and client ends were then obtained.
- Then, motor PID control was applied and the current, power, speed and torque changes on the client side were recorded.

Tests At Constant PWM Rate Of 80%

In the software, the ideal value for the PWM rate is 100% (i.e. a "1"), which corresponds to the numerical value of 1024. But, since we chose the PWM rate to be 80%, the number 818 has to be entered in the area of "Set Speed" in the server interface/ software.

Once the necessary settings were arranged, the load consisting of a series of lamps connected to the motor was gradually increased, and the torque and speed values noted, depending on changes in the motor current. The resulting graphs on the server side are shown in Figure 7.

It is observable that when the motor is loaded, current and torque increase, but the speed starts to decrease.

To observe the same values on the client side, the host-computer user has to push the "Allow Connection" button first, and the client-computer user has to operate the interface and enter the IP of the host computer into the settings tab, followed by pushing the "Connect" button. When the client computer begins to communicate with the system, the values in the "Motor Parameters" field will begin to change.

In some cases, there might be a difference between the values displayed on the server and client sides. This is the result of an unbalanced synchronization and communication loss when screenshots were taken.

It can be seen in Figure 8 that, at constant PWM, as long as the motor is loaded, the circuit's current and torque increase but motor speed decreases.

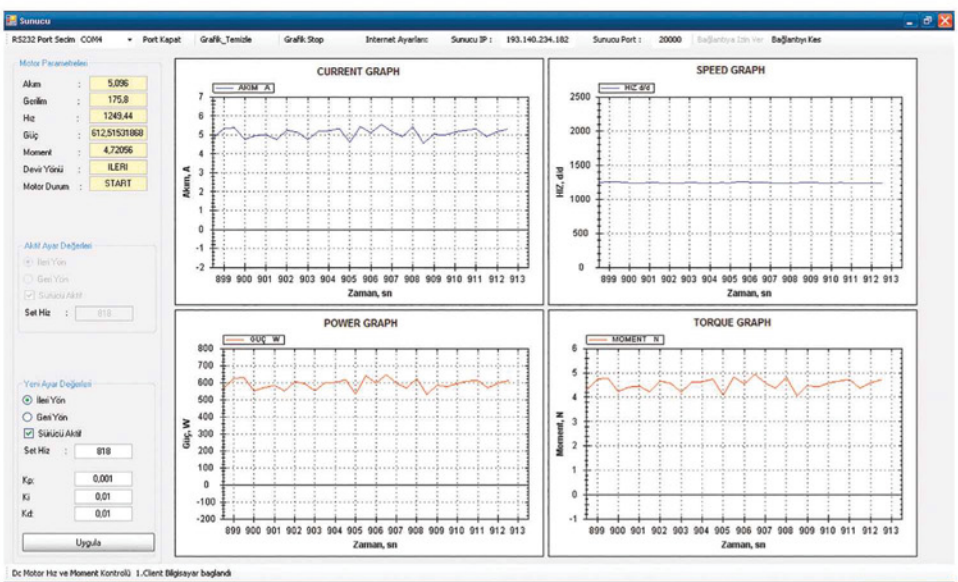

Figure 7: The graphs obtained for the server end, when the motor is at nominal load and PWM is 80%

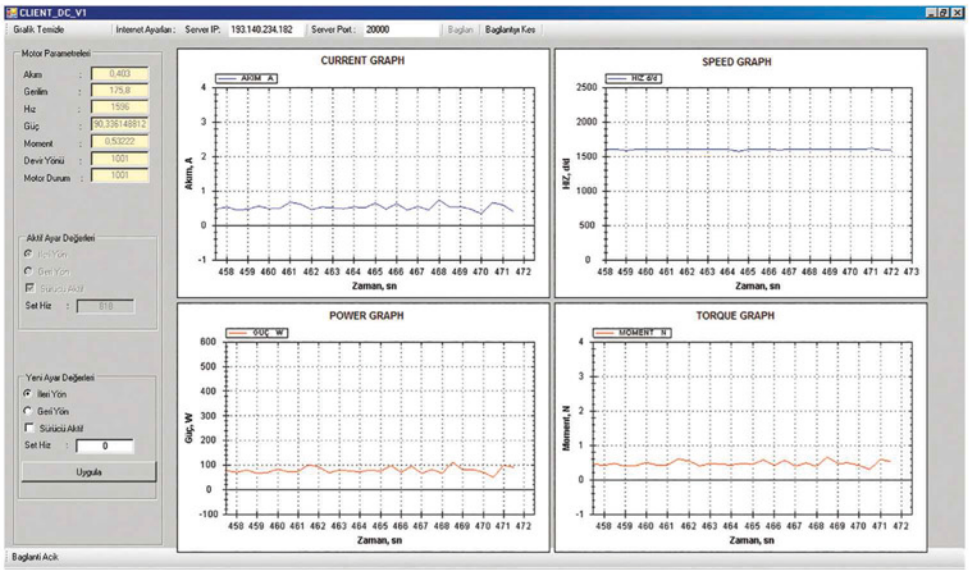

Figure 8: Graphs obtained on the client side when PWM is 80% and the motor is unloaded

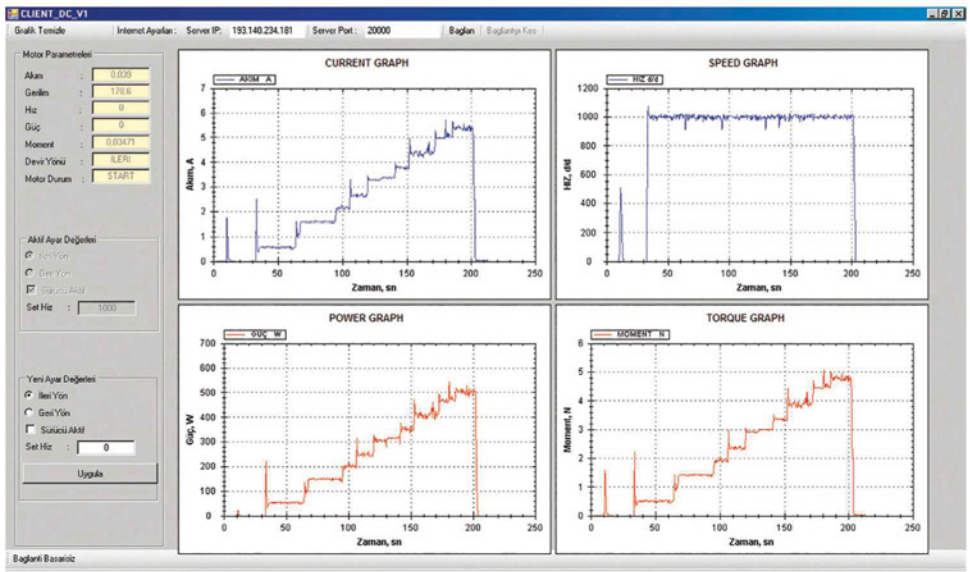

Figure 9: Graphs generated from PID control, obtained on the motor's client side

Implementing PID Control

When the speed of a DC machine needs to be changed in the 0-2000rpm speed range, it is not clear how long this operation will last. One method developed to keep steady operation at required level is PID control.

If a step function is applied to the input of the PID-control closed-cycle control system, the system will reach the new permanent state value as soon as possible.

Our PIC18F452 microprocessor communicates with the PC in series, and reads the direction of the rotation and speed of the DC motor from that PC. It reads the real speed of the DC motor from the tachogenerator and then operates the PID algorithm embedded in the microprocessor according to this data. Voltage is supplied to the motor via the PWM channel, and the data from the technogenerator is sent to the PC and displayed as a graph on its screen.

Graphs obtained on the client laptop side are shown in Figure 9. It can be determined that the speed remains constant at 1000rpm, when the motor to which the PID algorithm has been applied is loaded at certain levels. This confirms that the interaction between the designed interface and drive circuit works well.

It is important to note that control of the motor's speed and torque was carried out in real time without additional hardware. The decreasing costs of packet switched radio services suggest that the fast and safe control options provided by wireless systems will play a crucial role in future control system designs.

The most apparent feature that distinguishes this system from similar control systems is that provides a wireless remote monitoring solution that is economical and highly reliable.

MICROCONTROLLER-BASED STEPPER MOTOR CONTROL BASICS

PROFESSOR DOGAN IBRAHIM OF THE NEAR EAST UNIVERSITY IN CYPRUS DESCRIBES THE DESIGN OF STEPPER MOTOR CONTROLLERS

Stepper motors are brushless DC motors that rotate in small steps when excited. For example, a stepper motor with 360-step specification rotates only 1° when excited, while the direction of rotation depends on the type of excitation. The excitation is in the form of a pulse, and the motor advances after receiving a pulse.

Stepper motors operate in open-loop mode since they can hold the required position without any feedback sensors. Most stepper motors use permanent magnets and operate on the principle of attraction or repulsion between the rotor magnet and stator electromagnets.

Stepper motors are used in many industrial, commercial, domestic and educational applications because of their low cost, reliability and high torque at low speeds. Some common applications include printers, plotters, robotics, disk drives, drilling machines, grinding machines, laser cutting, sewing, medical devices and more.

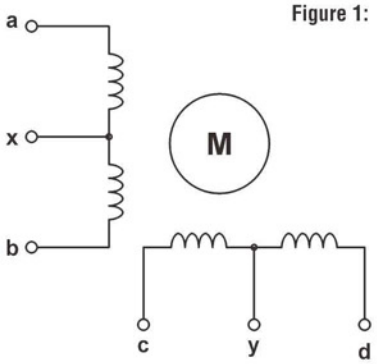

Figure 1: Unipolar stepper motor windings

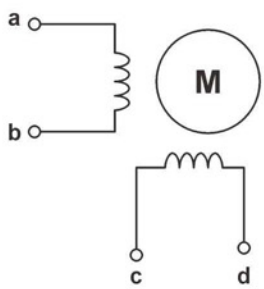

Figure 2: Bipolar stepper motor windings

The Pros And Cons Of Stepper Motors

The advantages of stepper motors are:

- Precise positioning and repeatability;
- High reliability (no contact brushes);
- Open-loop control, making the application simpler and less costly as there is no need for sensors;
- It is possible to achieve accurate low-speed rotation;
- 3-5% step angle accuracy with non-cumulative errors between steps;
- No stability problems;
- Full torque at low speed and at standstill (if energized);
- Excellent start-up response.

Stepper motors also have some disadvantages:

- Their speed is limited;
- Torque decreases considerably as the motor reaches its maximum speed;
- High vibration levels due to stepwise motion;
- Synchronisation may be broken when overloaded.

Stepper motors can be driven in three step modes depending on the type of controller used: full, half and microstep. In full-step mode the motor rotates one full step. For example, a motor with 200 rotor teeth rotates 1.8° for each full step applied; one pulse from the controller is equivalent to one step rotation.

In half-step mode the motor rotates half the distance. Thus, for the above example, the motor will require 400 steps per revolution and the motor will rotate 0.9° for each applied pulse. Half-step mode produces smoother motion than full-step mode, but at about 30% less torque.

Microstep mode further subdivides the step distance. For the above example, it is possible to divide each full step of 1.8° into 256 microsteps, thus resulting in 0.007°/step accuracy and 51,200 steps per revolution. Although microstepping provides accurate positioning of the motor's rotor, the torque is 30% less than in full-step mode.

Stepper motors are selected based on their torque-speed characteristics. These characteristics depend on the type of motor used, the excitation mode and the type of driver used. The motor produces maximum torque at standstill as long as it is energized. Acceleration is another parameter used in the selection process

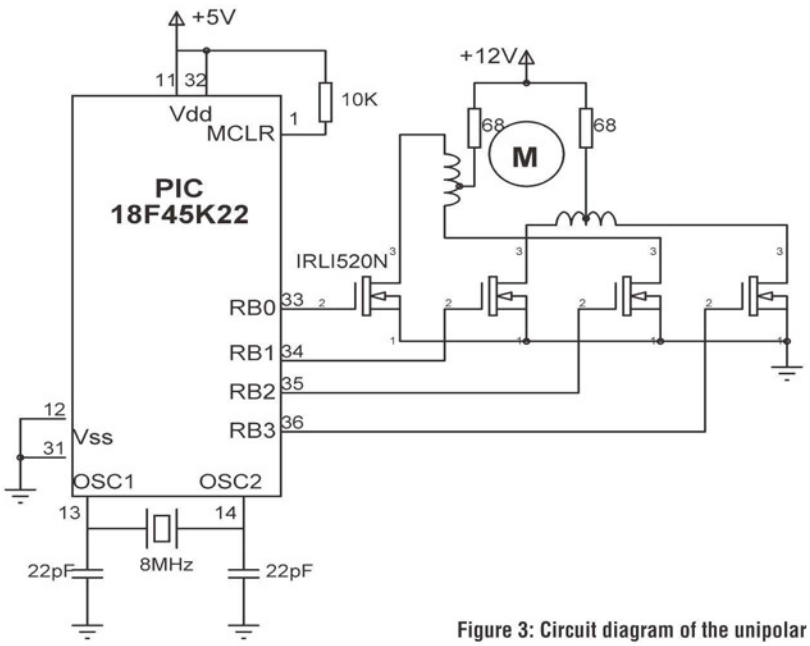

Figure 3: Circuit diagram of the unipolar stepper motor example

and is usually quoted as the time it takes for the rotor to move one step after the excitation.

In this article we will look at the control of both unipolar and bipolar stepper motors, and give microcontroller-based examples to demonstrate how these motors can be easily controlled.

Wiring Configurations

Stepper motors come in two basic wiring configurations: unipolar and bipolar.

Unipolar stepper motors have two identical and independent coils with centre taps, having five, six or eight wires (see Figure 1). This allows the motor direction to be reversed easily by changing which section of the phase is powered rather than reversing the flow of current, and requiring a very simple control circuitry.

Unipolar stepper motors can be driven in three modes: one-phase full-step sequencing, two-phase full-step sequencing and two-phase half-step sequencing.

Table 1 shows the sequence of sending pulses to the motor; each cycle consists of four pulses, and the motor rotates by one full step after each pulse.

Step	a	c	b	d
1	1	0	0	0
2	0	1	0	0
3	0	0	1	0
4	0	0	0	1

Table 1: One-phase full-step sequencing

Table 2 shows the sequence of sending pulses to the motor for two-phase full-step sequencing. The torque produced is higher in this mode of operation.

Step	a	c	b	d
1	1	0	0	1
2	1	1	0	0
3	0	1	1	0
4	0	0	1	1

Table 2: Two-phase full-step sequencing

Table 3 shows the sequence of pulses sent to the motor for two-phase half-step sequencing. This mode of operation gives more accurate control of the motor rotation, but requires twice as many pulses for each cycle.

Step	a	c	b	d
1	1	0	0	0
2	1	1	0	0
3	0	1	0	0
4	0	1	1	0
5	0	0	1	0
6	0	0	1	1
7	0	0	0	1
8	1	0	0	1

Table 3: Two-phase half-step sequencing

Unipolar motors are easily controlled with a microcontroller or dedicated controller chips, and are very affordable.

Bipolar Stepper Motors

Bipolar stepper motors have two identical and independent coils and four wires with no centre taps, as shown in Figure 2. In order to reverse the direction of rotation, the current direction is reversed. This requirement makes the driving circuitry more

```
const unsigned int Req_Rev_Count = 100;          // Required no of revs
const unsigned char Step_Size = 18;              // Motor Step Size (degrees)

void main()
{
unsigned char Step[4] = {1, 2, 4, 8};
unsigned int One_Rev_Step, Step_Count, Cycle_Count, j;
unsigned char i;
ANSELB = 0;                                      // Configure PORTB as digital
TRISB = 0;                                       // Configure PORTB as digital

One_Rev_Step = 360/Step_Size;                    // No of steps for 1 revolution
Step_Count = Req_Rev_Count*One_Rev_Step;         // Total no of steps required
Cycle_Count = Step_Count/4;                      // No of cycles

for(j = 0; j < Cycle_Count; j++)                 // Do for all cycles
{
for(i = 0; i < 4; i++)                           // Do for all steps
{
PORTB = Step[i];                                 // Send pulses to the motor
Delay_Ms(3);                                     // 3 ms delay between each pulse
}
}
while(1);                                        // End. Wait here forever
}
```

Figure 4: Program listing for simple unipolar stepper motor control

complicated and, as we will see later, is generally implemented with an H-bridge control circuit. Although more complicated to drive than unipolar motors, bipolar motors produce higher torques.

The control of bipolar stepper motors is slightly more complex. Table 4 shows the driving sequence. The "+" and "-" signs denote the polarity of the voltage applied to the motor legs.

Step	a	c	b	d
1	+	-	-	-
2	-	+	-	-
3	-	-	+	-
4	-	-	-	+

Table 4: Bipolar motor drive sequencing

Simple Unipolar Stepper Motor Drive Example

Here we give an example to show how a unipolar stepper motor can easily be controlled using a microcontroller. The motor is turned 100 revolutions and is then stopped.

The circuit diagram of the project is shown in Figure 3. The project uses a PIC18F45K22 microcontroller and a UAG2 unipolar stepping motor. The motor is connected to the RB0:RB3 pins of the microcontroller via IRLI520N power MOSFET transistors.

UAG2 is a small stepper motor with 18° stepping angle, where a complete revolution requires 20 pulses. In this example the motor rotates 100 turns (i.e. 2000 pulses are given) and then stops; 3ms delay is inserted between pulses to slow it down.

The program is based on the mikroC compiler; its listing is given in Figure 4. The motor operates in one-phase full-step sequencing mode. At the beginning of the program, the required number of revolutions and step size are defined. Inside the main program array 'STEP' stores the sequence of pulses to be sent to the motor in each cycle. PORTB is configured as digital output. Then, the cycle count is calculated and pulses sent to the motor inside two 'FOR' loops. The motor rotates 100 revolutions when 2000 pulses are sent to it; at 3ms delay between pulses, it operates for six seconds. Its speed can easily be calculated to be 1000rpm.

Complex Control Of A Unipolar Stepper Motor

In this example a unipolar stepper motor is controlled in the following manner:

- Turn 200 revolutions clockwise;
- Wait 5s;
- Turn 50 revolutions anticlockwise;
- Wait 3s;
- Turn 100 revolutions clockwise;
- Wait 1s;
- Stop.

The circuit diagram of the project is shown in Figure 5. In this example we use a UCN5804B stepper motor controller chip, which can drive small unipolar stepper motors up to +35V and 1.25A. The chip is connected to the microcontroller via its STEP and DIR pins. The chip also has half-step and phase selection inputs.

Depending on the connection of pins 9 and 10, the chip can operate in one-phase full-step, two-phase full-step, or two-phase half-step sequencing modes. In this project pins 9 and 10 are both connected to ground for two-phase full-step sequencing mode.

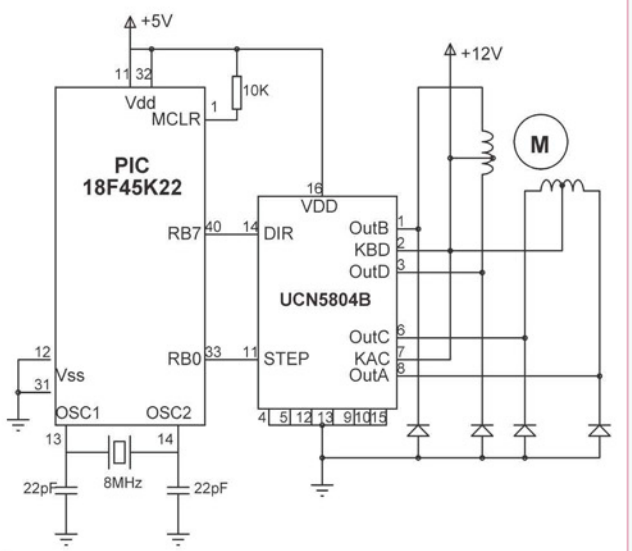

Figure 5: Circuit diagram of the project

The direction input controls the motor's direction. The motor rotates one step when a pulse is applied to the 'STEP' input. Notice that diodes are used at the output pins of the microcontroller to protect the pins from negative voltage.

The program listing is shown in Figure 6. The speed of a stepper motor depends on the time delay between step inputs. If the time delay between the steps is T and the motor step constant is ß degrees, then the motor rotates ß/T steps in a second. Since a complete revolution is 360°, the number of revolutions in a second is ß/360T. The number of revolutions per minute (rpm) of the motor is then given by:

RPM = 60ß/360T

or,

RPM = ß/6T

We can also write:

T = ß/6xRPM

In this project the motor has ß = 18°, so then:

T = 3/RPM, where T is in seconds

or,

T = 3000/RPM, where T is in ms.

If the required RPM is 500rpm (assuming this is below the maximum rpm that can be provided by the motor), then the delay between steps is:

T = 3000/500 = 6ms

Three arrays are used in the program to specify the required number of revolutions, the direction of rotation and the inter-step gap:

- **Rev_Count:** This array stores the required number of revolutions. A 0 entry specifies the end of the array. A negative value indicates that the motor is required to rotate continuously in the specified direction.
- **Rev_Direction:** This array stores the corresponding motor rotation direction; 0 for clockwise and 1 for anticlockwise rotation.
- **Inter_Delay:** This array stores the required delay after each command.

For the example in this project, the arrays should have the following values:

```
Rev_Count[ ] = {200, 50, 100, 0};          // 0 is the terminator
Rev_Direction[ ] = {0, 1, 0};              // 0 = clockwise, 1 = anticlockwise
Inter_Delay[ ] = {5000, 3000, 1000};       // Delay is in ms
```

At the beginning of the program, symbols 'STEP' and 'DIRECTION' are assigned to port pins RB0 and RB7 respectively. The arrays are then initialized, the step count is found, and a loop formed. Inside this loop the motor is activated by calling function 'Stepper_Motor'. This array has three arguments: revolution count, revolution direction and the delay after each command.

If the revolution count is negative, then the motor rotates continuously in the specified direction. The rotation stops when the revolution is specified as 0. The motor is rotated by setting the required direction and then sending pulses to the 'STEP' input of the UCN5804N controller chip.

```
#define STEP PORTB.RB0                          // UCN5804B Step input
#define DIRECTION PORTB.RB7                     // UCN5804B Direction input
const unsigned char Step_Size = 18;             // Motor Step Size (degrees)
const unsigned int RPM = 500;                   // Required RPM
unsigned int Step_Count, Delay;

void Stepper_Motor(int revcnt, unsigned char revdir, unsigned int gapdly)
{
unsigned int k,p;
if(revcnt < 0)
{
DIRECTION = revdir;
for(;;)
{
STEP = 1;                                       // Send pulse to the motor
STEP = 0;
VDelay_Ms(Delay);
}
}
else
{
p = revcnt*Step_Count;
DIRECTION = revdir;
for(k = 0; k < p; k++)
{
STEP = 1;                                       // Send pulse to the motor
STEP = 0;
VDelay_Ms(Delay);
}
for(k = 0; k < gapdly; k++)Delay_Ms(1);         // Inter command delay
}
}

void main()
{
int Rev_Count[] = {200, 50, 100, 0};                    // 0 is the terminator
unsigned char Rev_Direction[] = {0, 1, 0};              // 0=clockwise, 1=anticlockwise
unsigned char Inter_Delay[] = {5000, 3000, 1000};       // Delay in ms
unsigned char j;
ANSELB = 0;                                     // Configure PORTB as digital
TRISB = 0;                                      // Configure PORTB as digital
STEP = 0;                                       // Step = 0 to start with
j = 0;
Delay = 3000/RPM;                               // Delay after each command
Step_Count = 360/Step_Size;

while(Rev_Count[j] != 0)
{
Stepper_Motor(Rev_Count[j], Rev_Direction[j], Inter_Delay[j]);
j++;
}
while(1);                                       // End. Wait here forever
}
```

Figure 6: Complex unipolar motor control program

Simple Bipolar Stepper Motor Drive Example

This is a simple example showing how a bipolar stepper motor can be driven from a microcontroller. In this example, the motor is rotated 10 revolutions in one direction, then stopped for 5s, and then rotated 10 revolutions in the other direction, again then stopped.

The circuit diagram is shown in Figure 7.

In this project, an A3967SLB bipolar stepper motor controller chip is used. This chip can operate a stepper motor in the following modes, controlled by its MS1 and MS2 inputs:

- Full step;
- Half step;
- Quarter step;
- 8 microstep.

In this example the full step mode is used where MS1 = MS2 = 0.

The bipolar motor used in this project is the 39HS02, which has the following features:

- 1.8° step angle (200 steps for a complete revolution);
- ±5% step angle accuracy;
- 0.6A phase current;
- Four leads (coil 1: brown + gray, coil 2: orange + green).

The program listing is shown in Figure 8. At the beginning of the program the controller pins are defined by symbols. In the main program, the controller chip is enabled. Then a loop is formed to send 2000 steps (10 revolutions) to the motor in one direction (DIR = 0). After a 5s delay, the direction is changed (DIR = 1) and another 2000 steps are sent to the motor to rotate in the opposite direction. Notice that 1ms delay is inserted between steps so the speed of rotation is:
RPM = 1.8°/6 x 1 x 10 - 3s = 300. ●

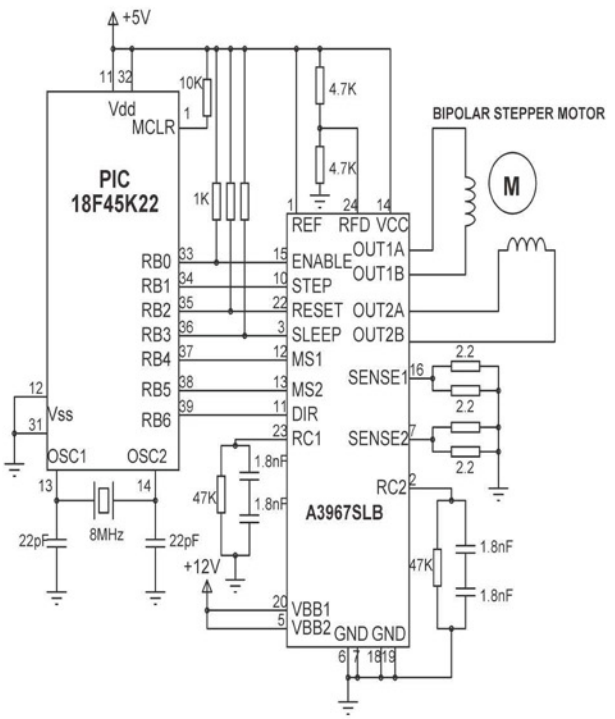

Figure 7: Circuit diagram for the bipolar example

```
#define ENABLE PORTB.RB0          // A3967SLB ENABLE input
#define STEP PORTB.RB1            // A3967SLB STEP input
#define RST PORTB.RB2             // A3967SLB RESET input
#define SLP PORTB.RB3             // A3967SLB SLEEP input
#define MS1 PORTB.RB4             // A3967SLB MS1 input
#define MS2 PORTB.RB5             // A3967SLB MS2 input
#define DIR PORTB.RB6             // A3967SLB DIR input

void main()
{
 unsigned int i;
 ANSELB = 0;                      // Configure PORTB as digital
 TRISB = 0;                       // Configure PORTB as digital
// A3967SLB chip configuration
 ENABLE = 0;                      // Enable the controller chip
 RST = 1;                         // Disable RESET
 SLP = 1;                         // Disable SLEEP
 MS1 = 0;                         // Full-step sequence
 MS2 = 0;
 STEP = 0;                        // Step = 0 to start with
// First rotate clockwise 10 revolutions
 DIR = 0;
 for(i = 0; i < 2000; i++)
 {
 STEP = 1;                        // Send STEP pulses
 STEP = 0;
 Delay_Ms(1);
 }
 Delay_Ms(5000);                  // Wait 5 seconds
// Now rotate anticlockwise 10 revolutions
 DIR = 1;
 for(i = 0; i < 2000; i++)
 {
 STEP = 1;                        // Send STEP pulses
 STEP = 0;
 Delay_Ms(1);
 }
 while(1);                        // End. Wait here forever
}
```

Figure 8: Bipolar stepper motor control program

OLSON®

POWER DISTRIBUTION UNITS

WITH LOCAL AND REMOTE POWER MONITORING

FOR DATA CENTRE 19" RACKS VERTICALLY MOUNTED WITH COMBINATION IEC 320 C13 AND IEC 320 C19 24-36 SOCKETS 230V 16AMP - 32AMP SINGLE PHASE

Since 1961 OLSON have specialised in the manufacture of mains distribution panels and is an established supplier to many leading UK Companies.

All OLSON units are manufactured to ISO9001 and with our quality management systems existing in all parts of our organisation, you can expect the very highest standard of service from first contact through to the despatch of each order.

CALL OUR SALES HOTLINE

020 8905 7273

Made in the UK

OLSON ELECTRONICS LIMITED

OLSON HOUSE, 490 HONEYPOT LANE, STANMORE, MIDDX HA7 1JY
TEL: 020 8905 7273 FAX: 020 8952 1232
e-mail: sales@olson.co.uk web site: http://www.olson.co.uk

3D-MIDs: THE NEW GENERATION OF CIRCUIT CARRIER DESIGN

BY **THOMAS HESS**, HEAD OF SALES AND PROJECT MANAGEMENT AT MULTIPLE DIMENSIONS

A three-dimensional moulded interconnect device, or 3D-MID, is an injection-molded thermoplastic part with integrated electronic circuit traces. The technology is the latest refinement and most recent high point in the history of circuit carrier design, extending the range beyond conventional rigid and flexible printed circuit boards (PCBs). With the benefits they offer, 3D-MIDs – sometimes simply called "MIDs" – are seeing a rapid increase in applications, from automotive and medical to consumer electronics, communications and even watchmaking.

History Will Tell

The first PCB patent and prototype were unveiled in 1925 by Charles Ducas and later by M. César Pasolini. The first one-sided PCB made an appearance in the 1950s, followed by double-sided construction with assembly. A patent for multi-layer PCBs was first outlined in the '60s, and 1982 saw the introduction of surface mount technology (SMT). In the '90s, the industry witnessed further developments with flexible and rigid-flexible PCBs. In 2014, global production value of the PCB industry reached $59.6bn, an increase of 3.7% on 2013.

3D-MID was first developed in the US in the 1970s with 2-shot (2K) plastics and hot-stamping as a method to make selected areas of a plastic component more amenable to chemical plating. Unlike PCB manufacturing, 3D-MID does not selectively remove copper from the surface; rather copper is added precisely where conductors are needed. In the 1990s, the new laser manufacturing (LDS) processes were developed in Europe and introduced a much broader capability for fine lines in 3D MID circuits. The first – and still leading – high-volume application is in antenna manufacturing for mobile phones, smartphones, tablets, and so on.

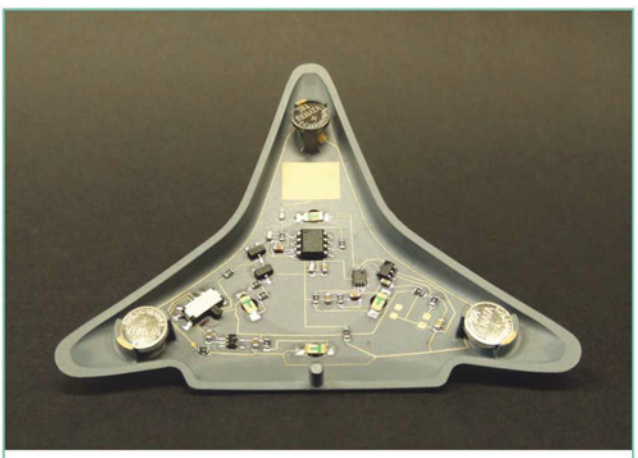

This Multiple Dimensions 3D-MID demonstrator includes various functions, including capacitive switch, battery holder, throughholes (diameter < 100µm) and a 3D electronic assembly

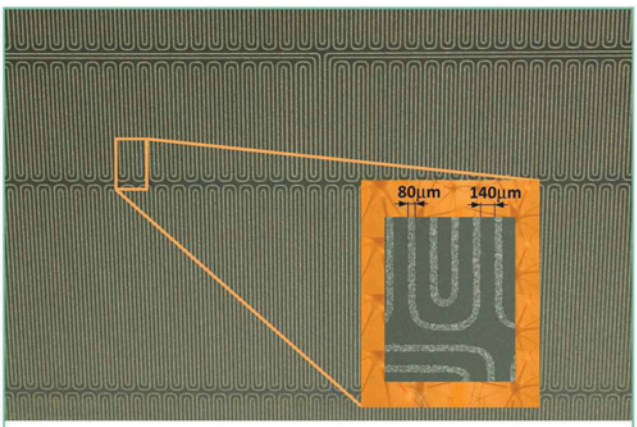

Multiple Dimensions can provide finest structures down to a line/space ratio of 80µm

Space-Saving Technology

3D-MID is a space-saving technology, one that also increases design freedom by eliminating the confinements of traditional two-dimensional PCB layouts and allowing for more electronic features in smaller volumes.

Designing in three dimensions allows electronic system modules and components to be uncomprimising in form and function. For example, it can revolutionize antenna designs; electrical noise shields can be placed exactly where needed at low cost, improving signals and isolating unwanted RF emissions; and LEDs and SMT components can easily be positioned in any orientation, which was previously expensive to implement in two-dimensional PCB structures.

Both mechanical and electronic functions can be tightly integrated into one part with construction that is much more compact, whilst also achieving greater density of functionalities.

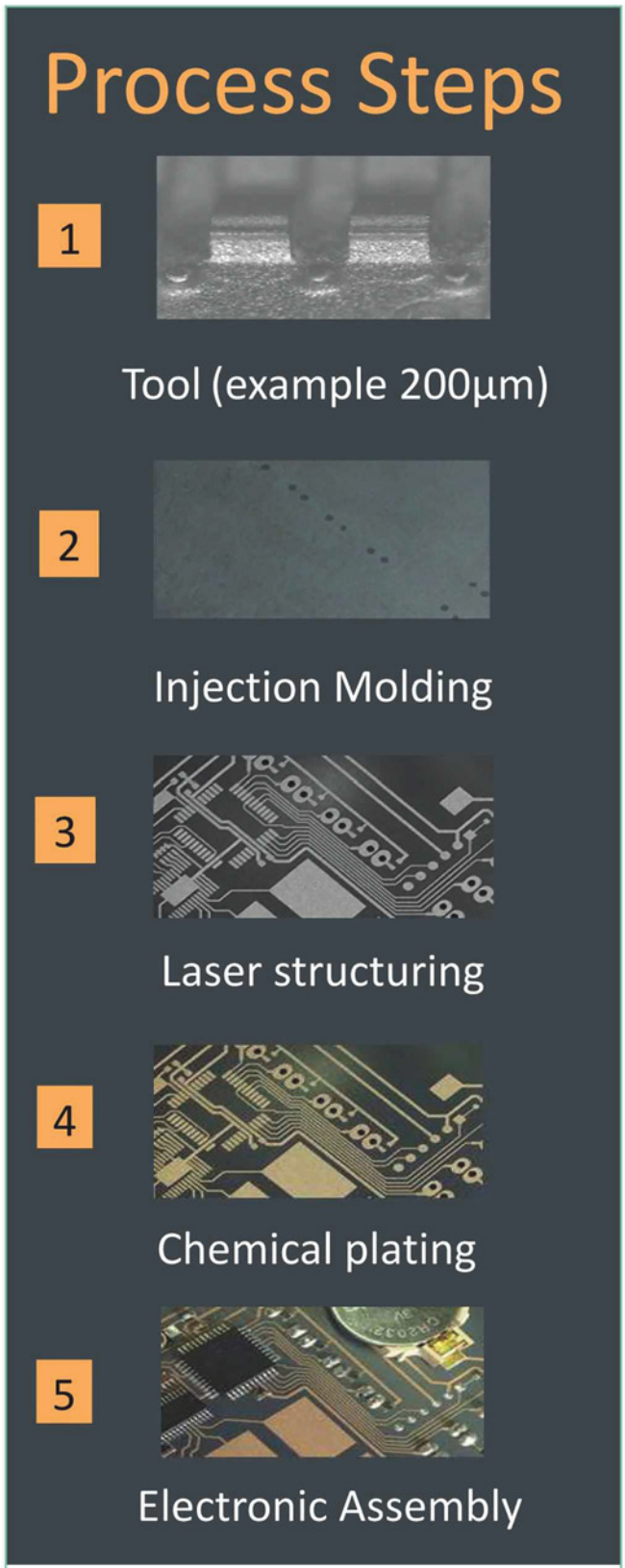

The five process steps in making a laser-structured circuit

With millions of smartphone antennas and automotive sensors already produced with 3D-MID annually, the attractions of 3D-MID are now expanding into many new application areas.

It's In The Package

There's a growing number of applications involving electrical and electro-optical circuits using 3D-MID technology. 3D packaging, package on package (PoP) and system in package (SiP) are just some of the packaging technologies that enable high functionality integration into the smallest of spaces. However, PoP or SiP deal with packaging on chip level, and the chip itself is assembled on the substrate, which is then electrically and mechanically connected to its functional environment.

Looking specifically at traditional ball grid arrays (BGAs) we see a good packaging method for dies that offers a small footprint and good heat dissipation. But, traditional BGAs also have disadvantages that can be addressed by 3D-MID. With 3D-MID construction the sensitivity to mechanical and thermal stress is lowered and thus failures are reduced.

Multiple Dimensions developed a processor housing with a selectively metallized molded part that eliminates the disadvantages of BGAs. In this solution the structure and contacts are one part – there's no interface and with no extra balls or pins, there are fewer components. With the 3D-MID component acting as carrier for the chip and the contacts, the package has lower mass, fewer components, is less complex and can be made thinner than conventional BGA packages.

Thermal management of the system is further improved with integration of heat sinks made with additional metallized surfaces on the substrate and/or and over-molded heat-sink inserts. Lateral connections to processors and other electronic components are possible with the substrate housing structured and metallized with additional traces and pads.

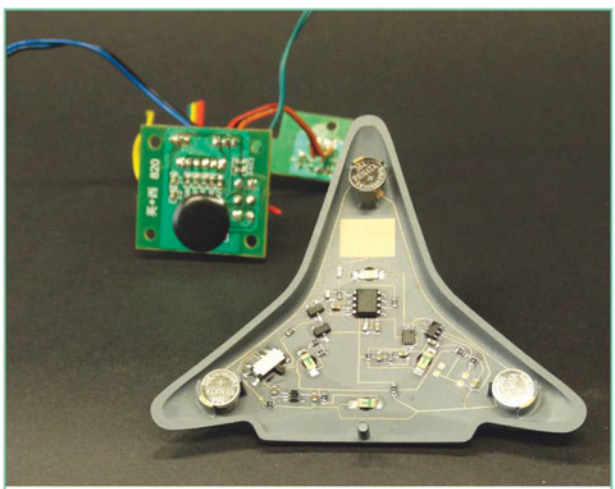

Injection molded interconnect devices are enjoying a rapid increase in applications

Multiple Dimensions is headquartered in Bruegg, Switzerland. Its current customer base consists of global companies in the industrial, medical, automotive, instrumentation and communications sectors

Manufacturing Processes

There are two main approaches to manufacturing 3D-MID products. One is laser direct structuring (LDS), a widely used and well-established process around the globe. With LDS, a single physical form is created with plastic injection molding, allowing any shape or form.

The molded thermoplastic contains a non-conducting organic-metal complex as an additive. As the laser scribes the desired circuit layout over the surface of the component, metal nuclei within the additive are activated, becoming attractive sites for plating. Chemical plating then applies copper, nickel and gold layers to transform the plastic part into a three-dimensional circuit carrier.

Multiple Dimensions is one of the dominant players on the market for the LDS process, but it now also produces 3D MID products using 2K, or the "2-shot" process. With 2K two different plastic materials are injection-molded side by side, with one material attractive to chemical plating and the other material more inert, acting as electrical insulator.

Enabling The Trends

The rapid adoption of the Internet of Things (IoT) concept is increasing the demand for MEMS too. According to the research institute HIS, worldwide sales of $16m in 2013 will jump to $120m in 2018. Applications will span across a variety of industries, from tracking systems to audio solutions and wearables, building automation and the smart grid.

Industry 4.0 is frequently described as the harbinger of the fourth industrial revolution. The networking of people, machines and the shop floor will transform production sites into smart factories. For this to happen, sensors are required to provide real-time information on the status of materials, temperatures, locations, and much more. Such sensors will be integrated into all objects, creating a productive workplace.

By integrating antenna structures directly on the MID-MEMS, data can be relayed directly from the sensor with no additional costly RF components. ●

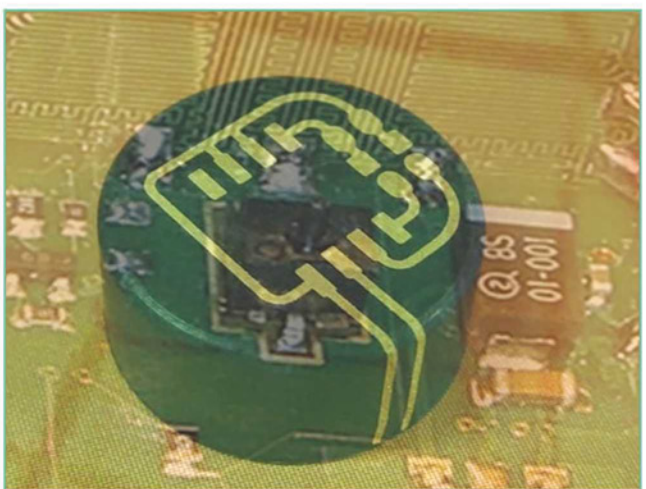

Injection molded sensor

MULTIPLE DIMENSIONS

Multiple Dimensions was founded by Dr Fritz Gantert, Johannes Schmid, Dr Roland Kuepfer and Nouhad Bachnak.

Currently, Multiple Dimensions is the leading independent 3D-MID manufacturer in Europe, producing many millions components per year.

Its second Galvanic Production Line was configured especially for metalizing the molded interconnected devices, based on the long experience of the experts at Multiple Dimensions. This line is regarded as the most modern of its kind.

The galvanic lines, together with high-tech lasers, fully-electric injection molding machines and additional systems form the modern production infrastructure at the site in Bruegg, Switzerland.

SPECIAL OFFERS
for full sales list
check our website

www.stewart-of-reading.co.uk

Check out our website, 1,000's of items in stock

Used Equipment – **GUARANTEED**
All items supplied as tested in our Lab
Prices plus Carriage and VAT

IFR 2025	Signal Generator 9kHz - 2.51GHZ Opt 04/11	£1,250
Fluke/Philips PM3092	Oscilloscope 2+2 Channel 200MHZ Delay etc	£295
HP34401A	Digital Multimeter 6.5 digit	£325
Agilent E4407B	Spectrum Analyser 100HZ - 26.5GHZ	£5,000
HP3325A	Synthesised Function Generator	£195
HP3561A	Dynamic Signal Analyser	£650
HP3581A	Wave Analyser 15HZ - 50KHZ	£250
HP3585B	Spectrum Analyser 20HZ - 40MHZ	£1,500
HP53131A	Universal Counter 3GHZ	£600
HP5361B	Pulse/Microwave Counter 26.5GHZ	£1,250
HP54600B	Oscilloscope 100MHZ 20MS/S	from £125
HP54615B	Oscilloscope 2 Channel 500MHZ 1GS/S	£650
HP6032A	PSU 0-60V 0-50A 1000W	£750
HP6622A	PSU 0-20V 4A Twice or 0-50V 2A Twice	£350
HP6624A	PSU 4 Outputs	£350
HP6632B	PSU 0-20V 0-5A	£195
HP6644A	PSU 0-60V 3.5A	£400
HP6654A	PSU 0-60V 0-9A	£500
HP8341A	Synthesised Sweep Generator 10MHZ-20GHZ	£2,000
HP83731A	Synthesised Signal Generator 1-20GHZ	£2,500
HP8484A	Power Sensor 0.01-18GHZ 3nW-10uW	£125
HP8560A	Spectrum Analyser Synthesised 50HZ - 2.9GHZ	£1,950
HP8560E	Spectrum Analyser Synthesised 30HZ - 2.9GHZ	£2,400
HP8563A	Spectrum Analyser Synthesised 9KHZ-22GHZ	£2,750
HP8566B	Spectrum Analsyer 100HZ-22GHZ	£1,600
HP8662A	RF Generator 10KHZ - 1280MHZ	£1,000
HP8970B	Noise Figure Meter	£750
HP33120A	Function Generator 100 microHZ-15MHZ - no moulding handle	£295
Marconi 2022E	Synthesised AM/FM Signal Generator 10KHZ-1.01GHZ	£325
Marconi 2024	Synthesised Signal Generator 9KHZ-2.4GHZ	£800
Marconi 2030	Synthesised Signal Generator 10KHZ-1.35GHZ	£750
Marconi 2305	Modulation Meter	£250
Marconi 2440	Counter 20GHZ	£295
Marconi 2945	Communications Test Set Various Options	£2,500
Marconi 2955	Radio Communications Test Set	£595
Marconi 2955A	Radio Communications Test Set	£725
Marconi 2955B	Radio Communications Test Set	£850
Marconi 6200	Microwave Test Set	£1,950
Marconi 6200A	Microwave Test Set 10MHZ-20GHZ	£2,500
Marconi 6200B	Microwave Test Set	£3,000
IFR 6204B	Microwave Test Set 40GHZ	£10,000
Marconi 6210	Reflection Analyser for 6200 Test Sets	£1,250
Marconi 6960B with	6910 Power Meter	£295
Marconi TF2167	RF Amplifier 50KHZ - 80MHZ 10W	£75
Tektronix TDS3012	Oscilloscope 2 Channel 100MHZ 1.25GS/S	£800
Tektronix 2430A	Oscilloscope Dual Trace 150MHZ 100MS/S	£350
Tektronix 2465B	Oscilloscope 4 Channel 400MHZ	£600
R&S APN62	Syn Function Generator 1HZ-260KHZ	£225
R&S DPSP	RF Step Attenuator 139dB	£300
R&S SMR40	Signal Generator 10MHZ - 40GHZ with Options	£13,000
Cirrus CL254	Sound Level Meter with Calibrator	£40
Farnell AP60/50	PSU 0-60V 0-50A 1KW Switch Mode	£195
Farnell H60/50	PSU 0-60V 0-50A	£500
Farnell B30/10	PSU 30V 10A Variable No Meters	£45
Farnell B30/20	PSU 30V 20A Variable No Meters	£75
Farnell XA35/2T	PSU 0-35V 0-2A Twice Digital	£75
Farnell LF1	Sine/sq Oscillator 10HZ-1MHZ	£45
Racal 1991	Counter/Timer 160MHZ 9 Digit	£150
Racal 2101	Counter 20GHZ LED	£295
Racal 9300	True RMS Millivoltmeter 5HZ-20MHZ etc	£45
Racal 9300B	As 9300	£75
Black Star Orion	Colour Bar Generator RGB & Video	£30
Black Star 1325	Counter Timer 1.3GHZ	£85
Ferrograph RTS2	Test Set	£50
Fluke 97	Scopemeter 2 Channel 50MHZ 25MS/S	£75
Fluke 99B	Scopemeter 2 Channel 100MHZ 5GS/S	£125
Fluke PM5420	TV Gen Multi Outputs	£600
Gould J3B	Sine/sq Oscillator 10HZ-100KHZ Low Distortion	£60
Gould OS250B	Oscillator Dual Trace 15MHZ	£50
Gigatronics 7100	Synthesised Signal Generator 10MHZ-20GHZ	£1,950
Panasonic VP7705A	Wow & Flutter Meter	£60
Panasonic VP8401B	TV Signal Generator Multi Outputs	£75
Pendulum CNT90	Timer Counter Analyser 20GHZ	£995
Seaward Nova	PAT Tester	£125
Solartron 7150	6 1/2 Digit DMM True RMS IEEE	£65
Solartron 7150 Plus	as 7150 plus Temp Measurement	£75
Solatron 7075	DMM 7 1/2 Digit	£60
Solatron 1253	Gain Phase Analyser 1mHZ-20KHZ	£750
Tasakago TM035-2	PSU 0-35V 0-2A 2 Meters	£30
Thurlby PL320	PSU 0-30V 0-2A Digital	£50
Thurlby TG210	Function Generator 0.002-2MHZ TTL etc Kenwood Badged	£65
Wavetek 296	Synthesised Function Generator 2 Channel 50MHZ	£450

STEWART OF READING
17A King Street, Mortimer, Near Reading, RG7 3RS
Telephone: 0118 933 1111• Fax: 0118 933 2375
9am – 5pm, Monday – Friday
Please check availability before ordering or **CALLING IN**

UK designed, UK made, *with pride.*

Tel. 01298 70012
www.peakelec.co.uk
sales@peakelec.co.uk

Atlas House, 2 Kiln Lane
Harpur Hill Business Park
Buxton, Derbyshire
SK17 9JL, UK

Follow us on twitter for tips, tricks and news.
@peakatlas

For insured UK delivery: Please add £3.00 inc VAT to the whole order. Check online or give us a call for overseas pricing.

PEAK® electronic design ltd

ZEN50 Zener Diode Analyser (inc. LEDs, TVSs etc)

Brand new product!

Introducing the new ***Atlas ZEN*** (model ZEN50) for testing Zeners (including Avalanche diodes) and many other components.

- **Measure Zener Voltage (from 0.00 up to 50.00V!)**
- **Measure Slope Resistance.**
- **Selectable test current: 2mA, 5mA, 10mA and 15mA.**
- **Very low duty cycle to minimise temperature rise.**
- **Continuous measurements.**
- **Single AAA battery (included) with very long battery life.**
- **Gold plated croc clips included.**
- **Can measure forward voltage of LEDs and LED strings too.**

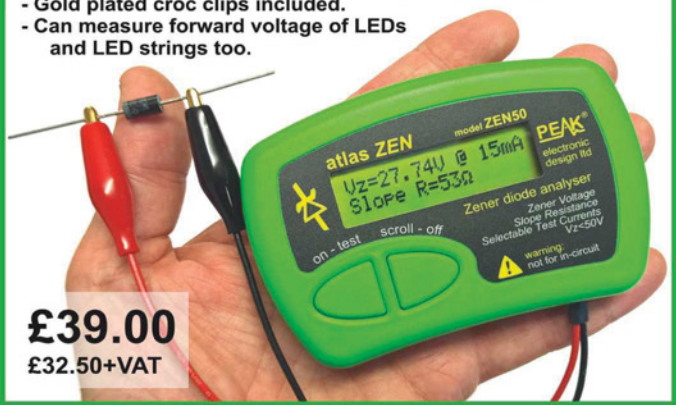

£39.00
£32.50+VAT

PCA23 SOT23 Test Adapter for Multimeters and Peak Analysers

Brand new product!

Designed to look like a giant SOT23 device, this beautiful adapter allows you to easily connect surface mount diodes, Zeners, MOSFETs and transistors.

Just place your device into the controlled-force clamshell and connect your probes to the gold plated test points.

Great for connecting crocs, hook-probes and multimeter prods.

£19.80
£16.50+VAT

DCA75 The famous DCA Pro

"A very capable analyser"
- Detailed review in RadCom magazine

Exciting new generation of semiconductor identifier and analyser. The ***DCA Pro*** features a new graphics display showing you detailed component schematics. Built-in USB offers amazing PC based features too such as curve tracing and detailed analysis in Excel. PC software supplied on a USB Flash Drive. Includes Alkaline AAA battery and comprehensive user guide.

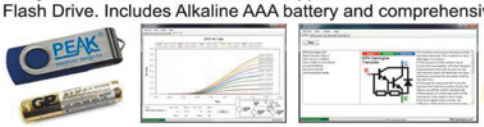

NEW LOW PRICE!
£105.00
£87.50+VAT

It's only possible to show summary specifications here. Please ask if you'd like detailed data. Further information is also available on our website. Product price refunded if you're not happy.

SURFACE MOUNT TECHNOLOGY ENHANCEMENTS IN 2015

BY **MULUGETA ABTEW**, VICE-PRESIDENT OF PROCESS TECHNOLOGY DEVELOPMENT AT SANMINA

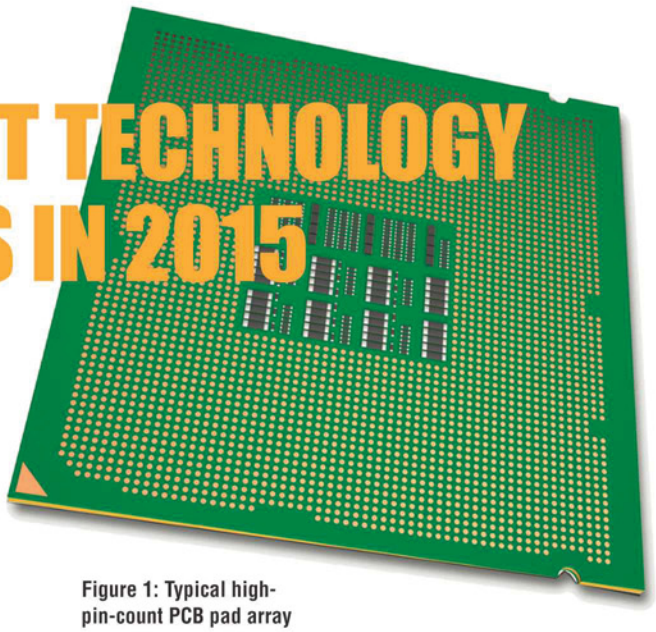

Figure 1: Typical high-pin-count PCB pad array

Nowadays, all industries demand greater functionality, complexity and miniaturization from their electronic devices. As a result, designers continue to face challenges relating to speed, bandwidth and new technologies in printed circuit boards (PCBs) and printed circuit board assemblies (PCBAs). Typically, innovations in PCB core technologies and PCBA processes largely depend on the Electronic Manufacturing Service (EMS) providers and the advancements they make.

Current Challenges

New components entering the market constantly drive the evolution in surface mount technology (SMT); ball grid array (BGA) devices with up to 3700 terminations are in production today. This is a significant increase in complexity when compared to the 64-pin BGAs from the early 1980s.

Bottom-terminated components (BTC) introduced in the 1990s with pin-counts of just a few dozen now have 200 to 300 pins. At the same time, the pad pitch of devices in production today has been reduced to 0.4mm – or smaller – compared to 1-1.5mm several years ago. A number of factors drive pad pitch limitations, including PCB via pitch, via technology (e.g. stacked vias) and line pitch currently between 2.5 and 3 mils for most production PCBs.

Today's complex designs with increased functionality and higher speeds need closer IC and component spacing, so PCB technology is being driven to minimize chip-to-chip spacing and yet keep signal integrity intact. EMS providers are working to solve key technology challenges for their OEM customers, including reducing the pitch between components while reserving sufficient space for rework; eliminating "head-on-pillow" defects in connections; minimizing voids in BTCs; and improving the robustness of PCBs used in high-temperature and/or corrosive industrial environments such as oil and gas exploration.

Component Spacing Reduction

OEMs are focused on functionality and performance. The use of decoupling capacitors for noise reduction leads to designs with more interconnects and smaller components, with tighter component spacing. New designs with more demanding signal integrity requirements can result in conflicts between layout requirements and what can be manufactured.

With conflicts between design requirements and process capability, rework is becoming a challenge. For some high-performance computing and telecommunications PCBAs the cost of a single PCBA may reach well over $15,000. Therefore, it is imperative that the assembly is not damaged during rework.

Furthermore, adequate spacing between components is also required to ensure that heat used for rework does not damage the solder joints of adjacent components, or the components themselves.

> While devices with pad pitches in the range of 0.3 mils are already being assembled with automated surface mount equipment, this pad pitch cannot be commonly used for high-pin-count devices due to limitations in PCB technology

While IPC standards do not provide strict requirements for component spacing, and current SMT assembly processes can accommodate tight spacings, experience shows that at least 200 mils of space should be left around large BGAs to allow for rework. OEMs are placing decoupling capacitors as close as 40 mils apart in order to optimize noise performance. Companies are working on processes and rework tools that make reliable, repeatable rework possible, without inducing secondary reflow or additional rework of adjacent components. Although current solutions offer spacings well below 200 mils, additional process development and tooling enhancements are necessary to achieve tighter component spacing.

IC Package Warpage

To minimize cost, ICs are often contained in plastic packages. However, plastic is less stable than ceramic, for example. When plastic packages are exposed to high temperatures during reflow, they can warp – 2 to 10 mils or more, depending on the substrate,

plastic material properties and package thickness and size. A combination of package and PCB substrate dynamic warpage, along with PCB pad solderablity issues and variations in printed solder paste volume can result in solder defects between a device and the PCB. Two common defects are head-on-pillow (HOP) and non-wet open (NWO) type defects.

While NWO defects create solder joints with no electrical continuity, HOP defects can be intermittent and/or unreliable. Therefore, testing for HOP defects is a challenge, so time-consuming and resource-intensive screening processes are needed to prevent these defects from getting into the field.

The JEDEC specification for package warpage, revised in 2005 and re-published in 2009, allows for a maximum 8 mils co-planarity at room temperature. Component suppliers usually provide specifications for room temperature co-planarity, using either the seating plane or regression plane measurement method. As long as the value is under 8 mils, co-planarity is deemed within specification.

Empirical data suggests that the JEDEC specification is no longer adequate. For high-pin-count packages with small pads and lower solder volumes, production data suggests that component warpage exceeding 3.5 mils can cause problems during reflow, with a high potential for HOP defects. Manufacturers of consumer devices may discard or recycle defective boards, but this is not an option for an advanced computing or communications PCBA costing thousands of dollars. Time-consuming and expensive 3D x-ray testing is necessary with assemblies susceptible to HOP defects.

In 2015, EMS providers will continue to drive changes – including advocating for improved plastic material compounds – along with JEDEC to tighten the standard warpage specification to closer to 3.5 mils for high-pin-count devices.

BTCs: Minimizing Voiding

PCBs with BTCs are increasingly common, as BTCs offer good performance – both in signal integrity and thermally – at a relatively low cost. However, increasing pin-count and package size, and reducing pitch on BTCs creates production challenges. The increased pin-count allows more functionality, and manufacturing faces new challenges in producing reliable contacts with these large-surface-area devices.

The biggest challenge with BTC packages is thermal pad voiding. During the solder reflow process, chemicals or air can be trapped in the solder, creating voids that may impact thermal conductivity or solder joint reliability. Large voids can result in early product failures or long-term reliability risks. Thermal pads present a unique challenge during reflow, since the pads are typically larger and connected to large copper areas within the PCB, they take longer to reflow than solder balls associated with signal pads. Stencil design techniques, soldering materials, new processes and design for manufacturability continue to minimize voiding. Vacuum reflow is also being investigated with promising results.

Assembly Of Rugged PCBAs

Industries such as oil and gas use electronic assemblies in very demanding environments. Drilling and exploration tools used two to three miles below the earth's surface operate in environments up to 350 degrees Farenheit and can cost over $2m. This equipment has to perform with precision, despite the high temperatures and pressures, vibration, mechanical shock and corrosive environments (oil, mud, moisture and chemicals). PCBAs deployed in these environments require high-temperature solders that are generally not suitable for current surface mount or automated pin through-hole manufacturing, so most of these PCBAs are still soldered manually.

Whilst high-lead solders are excluded from current RoHS legislation, there is interest in alternative high-temperature soldering materials, especially for environments up to 350 degrees Farenheit. This research is likely to continue beyond 2015, as OEMs and EMS companies work to develop better materials and processes.

Future Developments

SMT will continue to push the technical boundaries of signal integrity, miniaturization and increasing I/O counts. While devices with pad pitches in the range of 0.3 mils are already being assembled with automated surface mount equipment, this pad pitch cannot be commonly used for high-pin-count devices due to limitations in PCB technology (via escape) and package warp.

Vacuum soldering, which eliminates voids, will most likely enter the mainstream. Vacuum-assisted reflow soldering (vapor phase or modular reflow – which involves adding a vacuum zone) equipment currently costs 1.2 to 1.3 times more than conventional equipment. As equipment prices drop, vacuum soldering is likely to become more common.

Challenges seen in 2015 are not unlike those the electronics industry has faced over the past 10 years, but solutions will continue to require more advanced process technology and equipment. The result will be new processes, and PCB and PCBA technologies that would have been seen as unachievable just a few years ago. ●

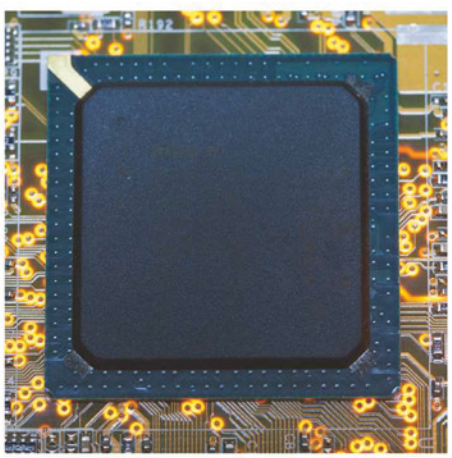

Figure 2: High pin-count BGA device

UNDERSTANDING COPPER DISSOLUTION AND SURFACE FINISH IN ROHS SELECTIVE SOLDER EQUIPMENT

BY **THOMAS SHOAF**, PROCESS ENGINEER AT PLEXUS

The challenges of achieving minimum vertical hole fill requirements on automated plated through hole (PTH) liquid soldering processes is well known to any manufacturer who has transitioned to lead-free solder. To successfully meet the hole fill requirement, enough energy must be supplied to the PCB to allow the liquid solder to flow to the top of the assembly before freezing. One successful method of achieving the required energy level is through thermal energy transfer management, either from a preheat process or from contact with liquid solder.

Balancing Act

Preheat of an assembly refers to applying a heat source just prior to the soldering process. Although a useful tool, its effectiveness is restricted due to flux chemistry limitations and some component thermal restrictions. Proper solder-joint formation only occurs if solder has a clean surface on the pin and barrel on which to make an intermetallic formation.

The effectiveness of flux is a function of time and temperature; the higher the temperature and longer the flux's exposure to heat, the less effective it is. This is an inverse relationship to the effectiveness of energy transferred to a PCB, where the hotter the assembly and the more time it has to thermally soak, the more effective the energy transfer. With this inverse relationship, a balancing act must be performed to ensure that enough thermal energy is transferred while maintaining flux effectiveness. This is made even more difficult by the use of no-clean fluxes, with relatively low activation temperatures, by increasing standards for cleanliness for clean and no-clean assemblies and by the increasing list of flux components found on the REACH list.

The same balancing act is required for components with thermal restrictions, where the thermal requirements of the PCB must balance the maximum temperature and time the component can survive without damage.

Contact with liquid solder can also transfer thermal energy into the PCB. The transition to lead-free solder has reduced the effectiveness of this method of energy transfer because of the increased dissolution rates of copper caused by lead-free alloys. In an effort to reduce this copper dissolution rate, lead-free alloys are superheated much less than tin lead alloys, reducing the flow and amount of energy loss required before solidification, resulting in a smaller viable process window for achieving complete vertical hole fill.

To maximize thermal transfer to the assembly and achieve adequate hole fill, without sacrificing the effectiveness of flux, increasing solder dwell time beyond six seconds and soldering

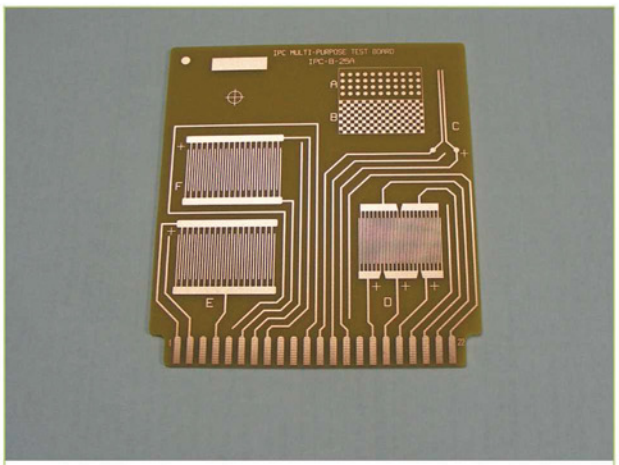

Figure 1: IPC-B-25 test board

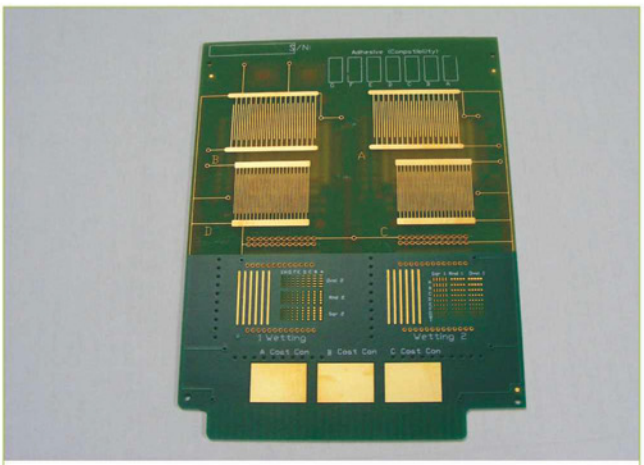

Figure 2: TV12 test PCB

VARIABLE	FACTOR 1	FACTOR 2
PCB Surface Finish	Bare Copper	ENIG
Solder Dwell Time	10 Seconds	20 Seconds
Solder Temperature	265°C	320°C

Table 1: Phase 1 variables

temperatures beyond 265°C were tested. To avoid negatively affecting joint quality, three phases of experimentation were conducted to understand the effect increased solder temperature and dwell time have on the dissolution rates of the base material (copper) of the solder joint.

Phase One

To understand the impacts of dwell times and solder temperatures that exceed the standard processing requirements on different surface finish types, two test vehicles were used. The first was a 0.5oz copper IPC-B-25A test board with bare copper finish (Figure 1); its test pattern was an IPC-B-24 test comb with 15mil trace width. The second vehicle was 1.0oz copper plated Plexus TV12 with ENIG (electroless nickel immersion gold) surface finish (Figure 2). The same IPC-B-24 test comb was also used on the second test vehicle.

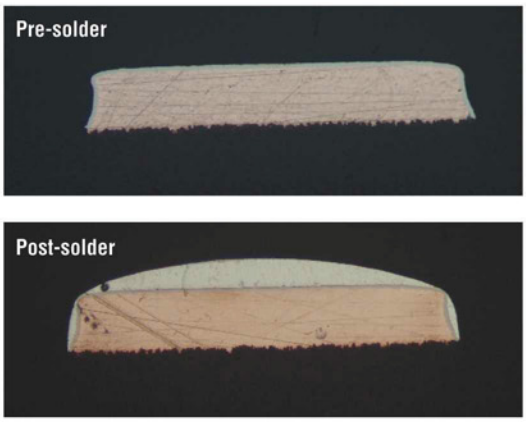

Figure 3: ENIG surface finish exposed to 320°C solder for 20s

The IPC-B-24 locations on the test vehicles were identified for testing because of consistent areas on both assemblies that mimicked surface-mount pads. They have been shown to have similar copper dissolution rates as the knee of PTH locations,

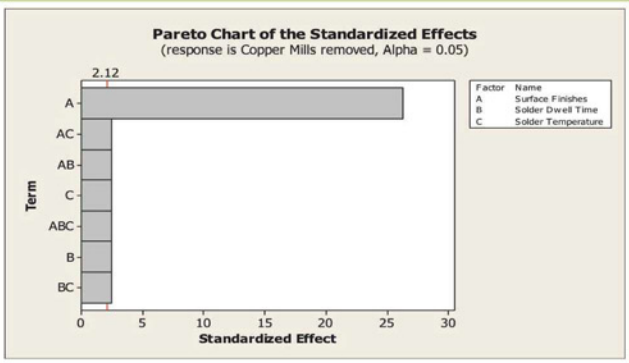

Figure 4: Phase 1 Pareto chart of the standardized effects

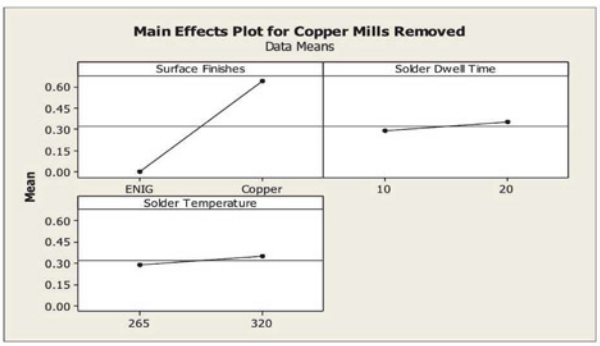

Figure 5: Phase 1 main effects plot for copper mils removed

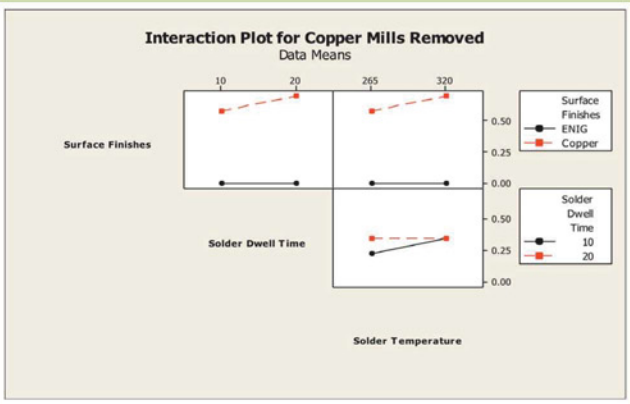

Figure 6: Phase 1 interaction plot for copper mils removed

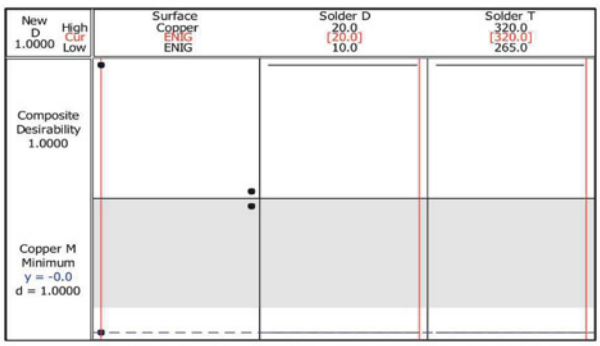

Figure 7: Phase 1 Optimization plot for copper dissolution with ENIG

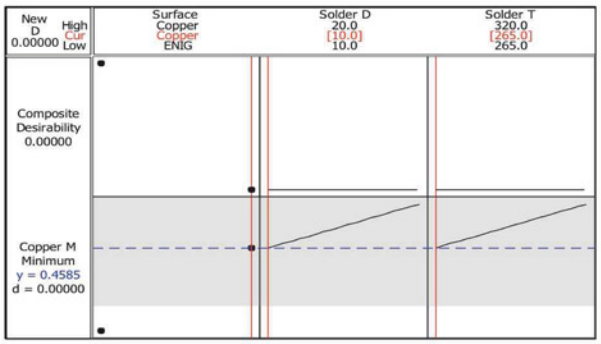

Figure 8: Phase 1 optimization plot for copper dissolution on bare copper

VARIABLE	FACTOR 1	FACTOR 2
PCB Surface Finish	Bare Copper	ENIG
Solder Dwell Time	2 Seconds	6 Seconds
Solder Temperature	265°C	320°C

Table 2: Phase 2 variables

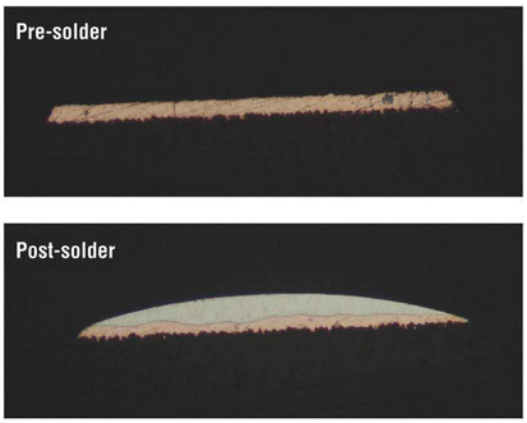

Figure 9: Bare copper surface finish exposed to 265°C solder for six seconds

arguably the most vulnerable portion of this solder joint.

The flux used for the design of experiments (DoE) was ORL0 no-clean flux and the solder was SAC305.

To understand the impacts of dwell time and solder temperature on different surface finish types, six variables were identified for testing (Table 1) and experimentation, structured as a full-factorial DoE completed in triplicate.

Six boards with four test locations each were used for 24 runs for the DoE. All experimentation was completed on an ERSA 50/60 selective solder using a universal selective solder pallet.

Processing constants used for the DoE were:

1. 130 micron flux head;
2. Flux spray time 1.5s;
3. Flux spray amount 40%;
4. 3mm x 6mm solder nozzle;
5. 75% solder flow;
6. Pull down 0.5s;
7. Solder pot Z height 1mm;
8. No preheat;
9. Transfer speed 60%.

Soldering on each test vehicle was completed at predetermined locations, and process conditions were completed as per the DoE structure. Solder pot temperatures were measured at the nozzle with a calibrated thermocouple, and recorded.

Cross-sectioning was completed at each test location and inspected at 20x magnification, and the thickness in mils of the remaining copper calculated using magnification image analysis software. A point on each cross-section, which was not exposed to solder, established the initial thickness of copper for the sample location. To calculate the mils of copper removed, the remainder was subtracted from the initial ones. This data was analyzed to determine the impact of dwell time, solder temperature and surface finish on copper dissolution.

A Pareto chart of the standardized effects with a 95% degree of confidence (Figure 4) and a main effects (Figure 5) plot showed surface finish has the greatest statistically significant effect on copper. Figure 4 demonstrates that all effects are statistically significant. An interaction plot (Figure 6) shows the interaction between solder dwell time and temperature.

An optimization plot (Figure 7) established the optimum dwell time and solder temperature on a copper/nickel surface finish. A maximum copper dissolution target was set to 0.14mils to allow for the potential rework of a 0.7mil, non-plated outer layer if these process conditions were used on production assemblies. With this maximum target the optimization plot provided mil copper dissolution with a solder dwell time of 20s and solder temperature of 320°C.

A second plot (Figure 8) was created to establish the optimum dwell time and solder temperature on a copper surface finish. With the same maximum target of 0.14mils of copper dissolution, the optimization plot established an optimum process at 10s of dwell time and 265°C solder temperature. The minimum copper dissolution was 0.45mils, well above the 0.14mils target.

Phase Two

Phase 2 was undertaken to understand the impacts of dwell times within the current requirements and solder temperatures within the standard processing requirements on different surface finish types.

The same test vehicles and test locations were used as with Phase 1. The flux used for the DoE was an ORL0 no-clean flux and the solder used was SAC305 alloy.

Six boards with four test locations each were used for 24 runs

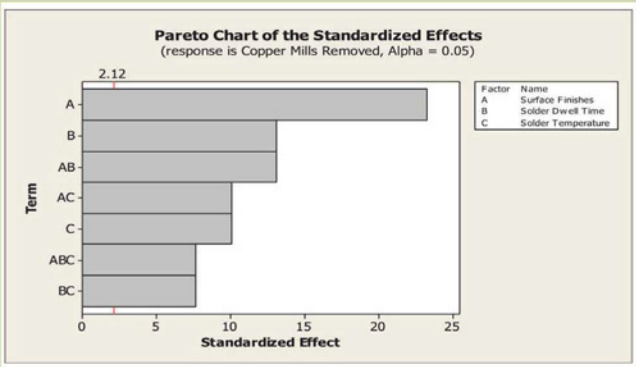

Figure 10: Phase 2 Pareto chart of standardized effects

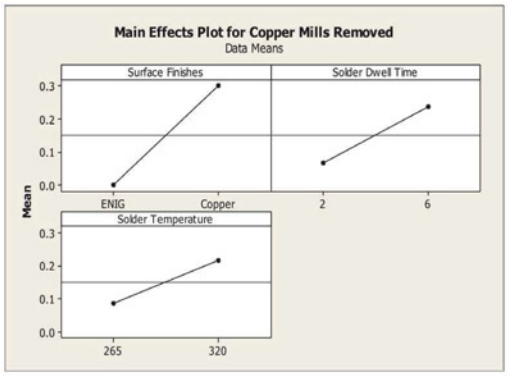

Figure 11: Phase 2 main effects plot for copper mils removed

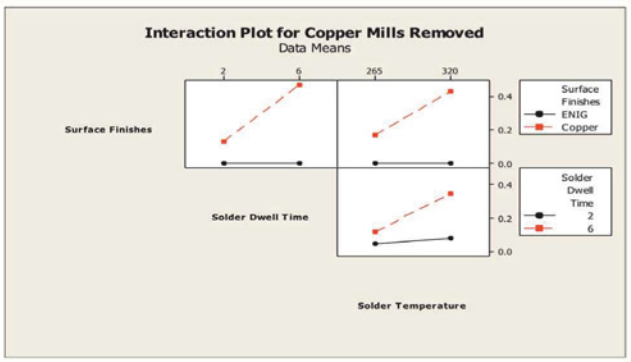

Figure 12: Phase 2 interaction plot for copper mils removed

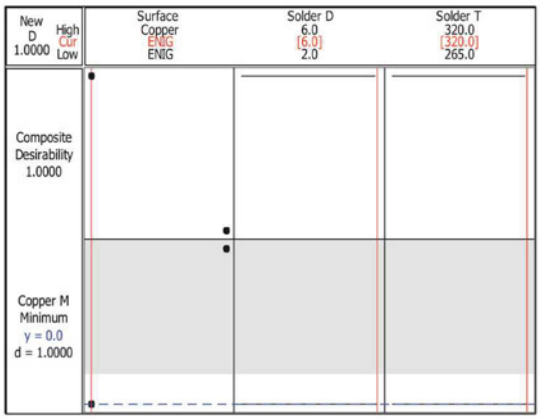

Figure 13: Phase 1 optimization plot for copper dissolution on ENIG

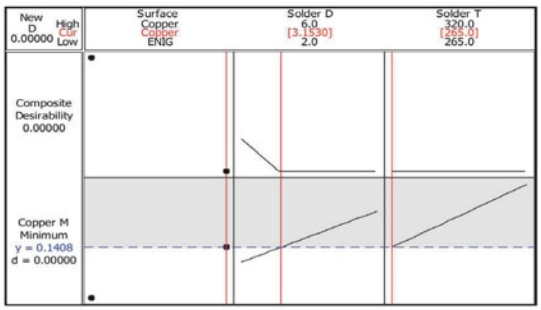

Figure 14: Phase 1 optimization plot for copper dissolution on bare copper

of the DoE. All experimentation was completed with ERSA 50/60 selective solder utilizing a Plexus selective solder universal pallet. Processing constants used were the same as Phase 1.

Inspection was carried out consistent with Phase 1.

A Pareto chart of the standardized effects with a 95% degree of confidence (Figure 10) and a main effects plot (Figure 11) showed all factors and combinations thereof to have statistical significance on copper dissolution. Surface finish, followed by solder dwell time, were most statistically significant factors. Interaction plot (Figure 12) showed no interaction of any factors in the process parameters tested.

An optimization plot (Figure 13) established the optimum dwell time and solder temperature on a copper/nickel surface finish. A maximum copper dissolution target was set at 0.14mils to allow for potential rework if these conditions were used on production assemblies. With this maximum target, the optimization plot was able to achieve a 0-mil reduction in copper when using a solder dwell time of 6s and solder temperature of 320ºC. Optimum temperatures and time established fall in line with Phase 1 results.

A second optimization plot (Figure 14) established the optimum dwell time and solder temperature on a copper surface finish. With a maximum target set to 0.14mils of copper dissolution, an optimum process at 3.15s of dwell time and 265ºC solder temperature was established. The minimum copper dissolution was 0.14mils, matching the target condition.

Phase Three

Phase 3 was carried out to explore the effects of solder temperature on a copper surface finish assembly at a common maximum dwell time using a Reptron Manufacturing card with

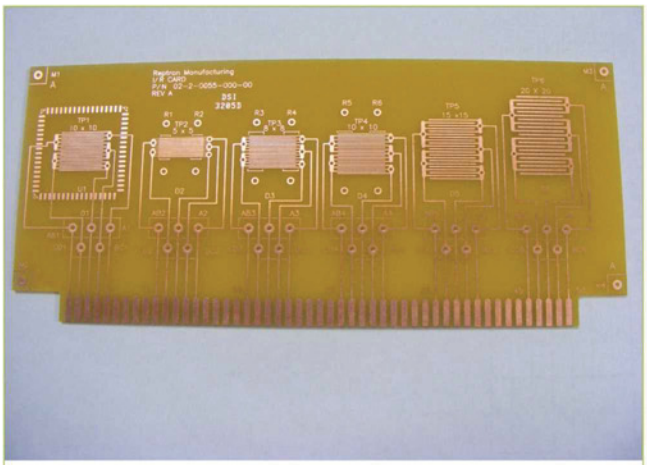

Figure 15: Reptron Manufacturing test board

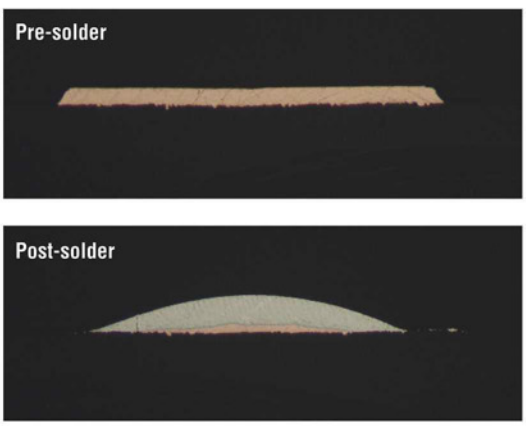

Figure 16: Bare copper surface finish exposed to 315ºC solder for six seconds

a bare copper finish (Figure 15), and test location on each card containing a 0.5oz honeycomb test pattern with 15mil trace-width. The flux used was an ORL0 no-clean flux and the solder was SAC305.

The factor for this ladder study was solder temperature at:

1. 265ºC;
2. 275ºC;
3. 285ºC;
4. 295ºC;
5. 305 ºC;
6. 215ºC.

This was completed with three replications of each solder temperature. Nine boards with two test locations each were used for 18 runs. All experimentation was completed on ERSA 50/60 selective solder using a universal selective solder pallet.

Processing constants used were:

1. 130-micron flux head;
2. Flux spray time 1.5s;
3. Flux spray amount 40%;
4. 3mm x 6mm solder nozzle;
5. 75% solder flow;
6. Pull down 0.5s;
7. Solder pot Z height 1mm;
8. No preheat;
9. Transfer speed 60%;
10. Dwell time 6s;
11. Bare copper traces.

All process conditions followed a predefined structure, and solder pot temperatures were measured at the nozzle with a calibrated thermocouple. Inspection was conducted as before.

All data points were entered into a scatter plot, and a linear regression line was calculated for analysis (Figure 17). This line shows that a 6s dwell time with a solder temperature of 265ºC yields a copper dissolution of 0.212mils; at 285ºC the copper dissolution is 0.366mils, and at 315ºC it is 0.597mils.

An average of all measurements at a specific solder temperature was divided by the dwell time (six seconds) to calculate a copper dissolution rate in mils per second for each solder temperature. The data was entered into a scatter plot and a linear regression line was calculated (Figure 18). This line demonstrates that at 265ºC the copper dissolution is 0.039mils per second, with an increase of 0.013mils dissolved for every 10ºC increase in temperature.

For verification of this data, the linear regression line equation in Figure 18 was used to determine a theoretical copper dissolution of a bare copper trace at 265ºC and 320ºC solder temperature. The theoretical values were compared to actual measured values of each dwell time on bare copper at 265ºC and 320ºC solder temperature (Figure 19). Considering the thermal mass difference between Phases 2 and 3 test vehicles, all measured and theoretical values and measured values were deemed similar.

Introduction Of Error

After data analysis was completed, two observations were made which could have introduced error into the data collection. To have two different surface finishes available for testing in Phases 1 and 2 required two different test vehicle designs with IPC-B-24 test locations. Two separate test vehicle designs create a difference thermal conductivity and thermal mass. With these particular test vehicle designs, the difference in thermal conductivity and mass should have minimal effect, but there is the potential for introduced error and affected dissolution rates.

In addition, the test vehicles used in Phase 1 and 2 had different initial finished copper thicknesses. This would cause a difference in thermal loading between the test locations, with the potential to affect the data analysis.

Conclusion

Clearly, surface finish selection is the most statistically significant variable affecting copper dissolutions. Of the surface finishes tested, ENIG outperformed bare copper in reducing dissolution with increase solder temperatures and dwell times.

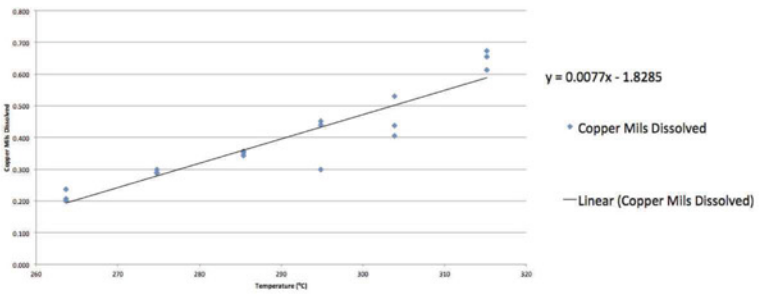

Figure 17: Phase 3 temperature vs mils dissolved

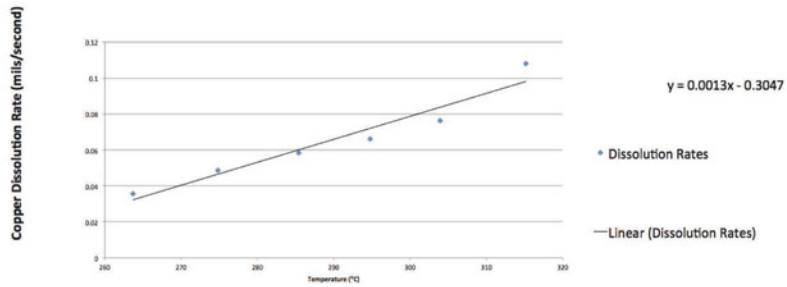

Figure 18: Phase 3 average copper dissolution rates

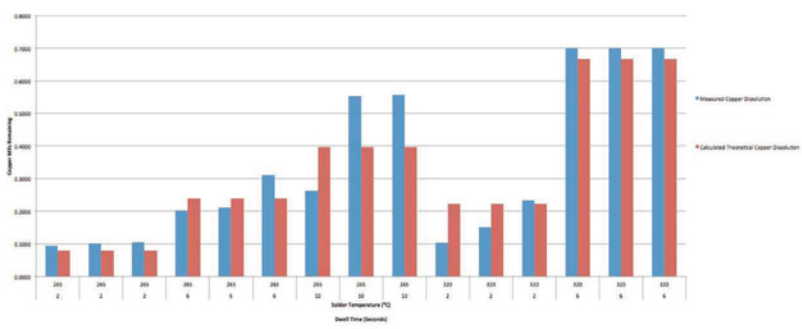

Figure 19: Measured vs calculated copper dissolution

Phase 1 determined that the ENIG surface finish could withstand increased solder dwell times of at least 20s, and solder temperature of at least 320°C without dissolution of copper. There is potential to explore further the use of increased dwell times and solder temperatures on high thermal mass assemblies with copper/nickel surface finish such as ENIG when soldering with SAC305.

Phase 1 and 2 demonstrated that copper dissolution of copper surface finishes increases when exposed to increasing SAC 305 solder temperatures and dwell times. To limit copper dissolution to 0.14mils the maximum solder temperature will need to be 265°C at 3.15s of dwell time.

Phase 3 defined that copper dissolution as a function of solder temperature has a linear relationship. It shows a 0.013mil per second increase in copper dissolution for every 10°C increase in SAC 305 solder temperature. This was verified by the theoretical copper dissolution values to measured values of bare copper test in Phase 2.

The calculated linear regression equation (Figure 18) showed temperature 265°C yields a copper dissolution rate of 0.039 copper mils per second. The theoretical value closely matches the measured values and is similar to previous test results. This supports the optimization model, leading to the conclusion that increasing solder temperature and solder dwell time beyond 265°C and six seconds is not recommend if maximum allowable copper dissolution is anywhere from 0.14 to 0.24mils.

By increasing the maximum copper dissolution of a bare copper surface finished PCB to 0.315mils, a roughly 20% reduction in the finished surface copper thickness of a PTH pad with a starting copper thickness of 0.5oz (1.7mils), the maximum solder dwell time and/or the solder temperature could be increased. At 0.315mils the linear regression equation calculated (Figure 18) predicts that solder temperature could be increased to 275°C at six seconds dwell time. Using a copper dissolution rate of solder at 265°C the solder dwell time can be achieved to 7.9s, with combinations in between. Increasing the allowable copper dissolution would require any internal standards regarding the quantity and duration of rework cycles to be reviewed and revised.

An understanding of the relationships explained here will provide a proven basis for anyone developing their own soldering procedures using current-generation materials and components and will, typically, reduce production ramp-time while reducing or eliminating solder-related failures. ●

RIGOL
Beyond Measure

Typical RIGOL:
Complete Oscilloscope Line
DS/MSO at affordable prices!

DS1054Z
Digital Oscilloscope
Best Price: from € 339,- plus VAT

- 50MHz, 12 Mpts Memory (optional 24Mpts)
- 4 Analog Channels, 1 GS/sec.
- Options: Decode, Trigger, Memory, Recorder

DS1000Z (-S) *PLUS*
Digital Oscilloscope
Best Price: from € 539,- plus VAT
NEW

DS1000Z Series as MSO READY

- 70/100MHZ Bandwidth, 4 Ch., 1 GS/sec.
- MSO 16 dig. IO, 1GS/ch, 12Mpts Memory
- Option: RPL 1116 Adapter, 16 IO's

DS/MSO2000A (-S)
Digital Oscilloscope
Best Price: from € 795,- plus VAT

PROMOTION UNTIL 31.12.2015:
All options included with purchasing a new MSO/DS2000A device

- 70/100/200/300MHz, 28Mpts (56Mpts) Memory
- 2 Analog Channels, 2 GS/sec
- As MSO: 16 dig. Channels, 1GS/ch, 14Mpts Memory

DS/MSO4000
Digital Oscilloscope
Best Price: from € 1.795,- plus VAT

- 100/200/350/500MHz, 140Mpts Memory
- 2 or 4 Analog Channels, 4GS/sec
- As MSO: 16 dig. Channels,1GS/ch, 28Mpts Memory

ALL OPTIONS AT THE PRICE OF ONE:
BND-MSO/DS4000 complete from € 549,00 plus VAT

More details at www.rigol.eu

RIGOL Technologies EU GmbH
Phone +49 89 8941895-0
info-europe@rigol.com
DISTRIBUTION PARTNERS:
www.rigol.eu/sales

RELEC ELECTRONICS LTD

Trying to keep a low profile?

Ranging from 40W to 112.5W with convection cooling and up to 225W with forced air cooling. Relec Electronics has a range of open frame ac dc power supplies on a 4" x 2" footprint with a height profile of just 25.4mm for those designs where a low profile is critical. All feature high efficiency with low standby power consumption and a universal ac input. Single fixed outputs range from 12 to 48Vdc on the lower power units and 12 to 58Vdc on the 112.5/225W unit.

Approved to IEC, EN, UL 60950-1 2nd edition, class II safety standards, the 40W & 60W PSU's have an optional function ground enabling them to meet class I when this is connected. Hold up time is between 10 and 16ms; the outputs are fully protected against over voltage and short circuits.

These power supplies are ideally suited for telecom, datacom and a wide range of industrial applications. For further information on the 40W **MPE-S040**, 60W **MPE-T060** or 112.5/225W **ABC225** series, view the Relec website or contact us directly.

Design solutions for design engineers

Relec Electronics Ltd
Tel: 01929 555800
e-mail: sales@relec.co.uk

www.relec.co.uk

Figure 1: Simplified view of the project

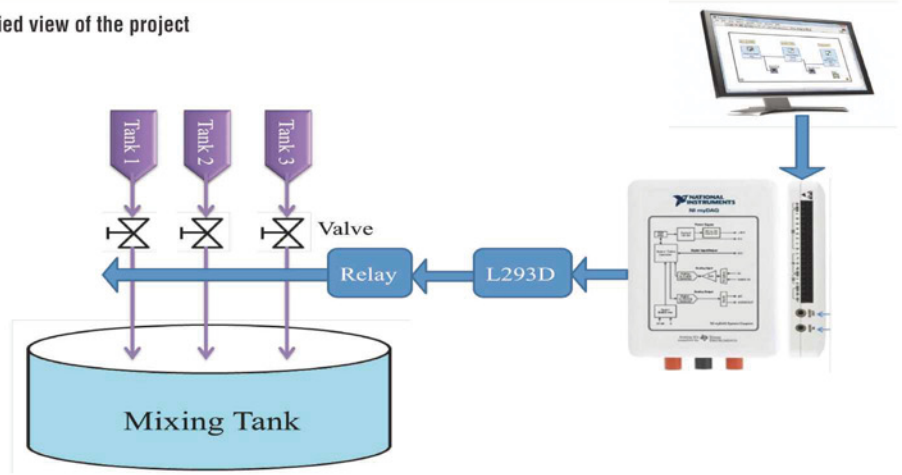

CHEMICAL MIXING WITH LABVIEW

BY **ASHISH PATEL, DEVANAND MAKWANA, JITENDRA AHUJA** AND **PROFESSOR ARJAV BAVARVA**
FROM RK UNIVERSITY IN INDIA

Industries have widely adopted automation, especially when it offers scalability, efficiency, accuracy, reliability and low power.

One aspect suitable for automation is the accurate mixing of chemicals required in many industries, among them food and pharma. Manual control can lead to improper dosing and mixing, which results in non-homogenous product in various ways, including chemical composition, colour, texture, flavour, reactivity and particle size. We developed our project to avoid such effects.

The aim was to introduce a systematic approach to the design and implementation of a volume-based chemical mixing system using LabVIEW (Laboratory Virtual Instrumentation Engineering Workbench) and National Instruments's (NI) myDAQ interface – a real-time fully-automated control system. LabVIEW is the platform and development environment for a visual programming language from NI. It is commonly used for data acquisition, instrument control and industrial automation; its code files have the extension '.vi', the abbreviation for 'virtual instrument'.

To mix the chemicals in a required ratio for example, a control signal is generated by LabVIEW and sent to myDAQ, which then actuates the mixing plant's valve relays accordingly.

Hardware Setup

Figures 1 and 2 show a simplified view of the project and block diagram respectively, where LabVIEW provides the graphical user interface (GUI). MyDAQ is a data acquisition device that allows measuring and analyzing real signals. Three solenoid valves are actuated in response to the control signals sent from LabVIEW via myDAQ, which is the interface. For digital output, porto is selected and line7/line6/line5 of porto is used. MyDAQ will operate an L293D motor driver IC, boosting its voltage as it drives the 12V DC relay and turns ON the respective valve.

The architecture shows three tanks for chemical filling and one common mixing container that houses the mixed chemical.

Figure 2: Project block diagram

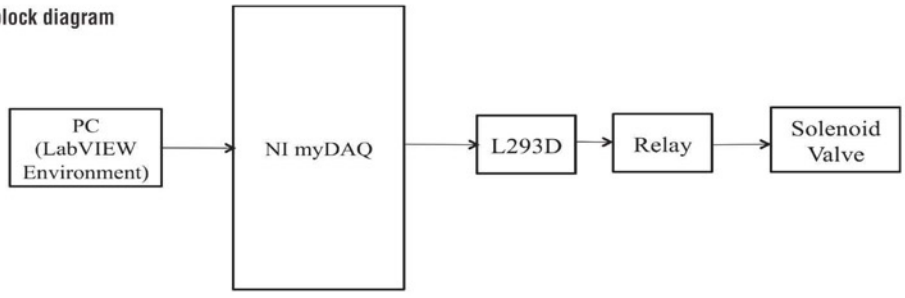

The Virtual Instrument

Figure 3 shows the main VI for the project that is made up of a flat sequential structure, executing steps in sequence, one by one. Sections 1, 2 and 3 operate valves 1, 2 and 3 respectively. Valve 1 is operated for a precise period of time that's been input in the 'Tank 1' field. As shown in Figure 3, N represents the total number of times the 'FOR' loop will iterate. The value of i shows the current iteration number, which starts from 0 and increments by one after each iteration.

"Wait until Next ms Multiple" (Figure 4) defines the time delay between two iterations. The "Greater?" logic block checks if N is greater than i. An LED or the valve turn off when N is below the value of i. Otherwise, the LED or valve remain on until N and 'Tank 1' are the same value. Because the 'Tank 1' value is given as an input to the "Wait until Next ms Multiple" (the delay between two iterations in milliseconds), the loop will iterate 1000 times (1s = 1000ms).

LabVIEW is a virtual platform, easily interfaced with real external hardware by following certain steps. Those steps include:
(1) create task;
(2) configure task;
(3) start task;
(4) acquire or generate data;
(5) clear task; and
(6) check for errors.

Tasks can be created by the DAQmx physical channel or virtual channel. DAQmx physical channel is used to select the hardware port (interface port of myDAQ that connects the my DAQ hardware to a PC via a USB cable).

DAQmx creates a virtual channel for generating digital signals. Here, a virtual channel is used as digital signal is generated from software. 'DAQmx Starts Task' receives the generated digital signals from 'DAQmx Create Virtual Channel'. 'DAQmx Write' writes or stores a signal from a selected port. This signal will be Boolean (true or false) since it is the output generated by the 'greater than' logical block. 'DAQmx Clear Task' clears the task. 'Simple Error Handler' indicates an error if one has occurred during execution of the previous block. At the end the 'dialog box' is used to display the error.

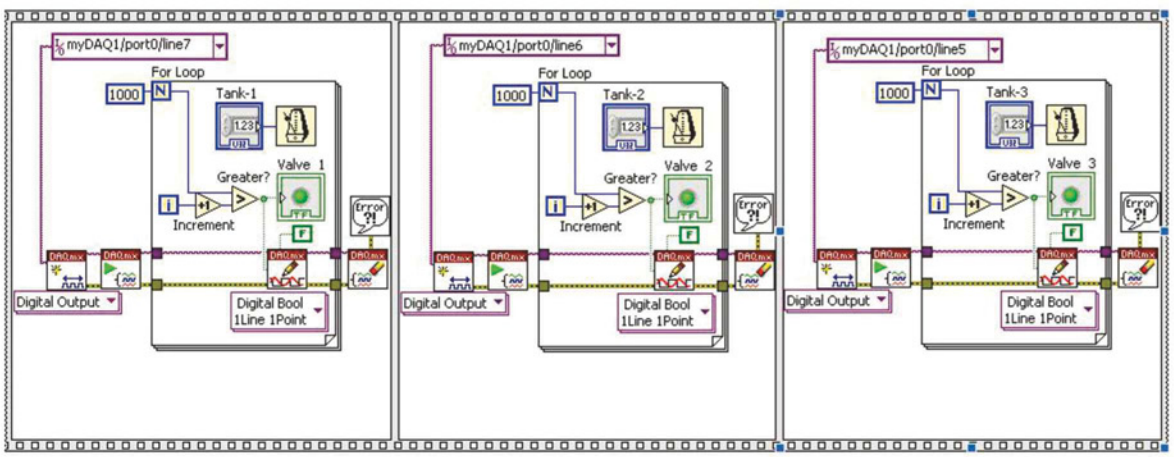

Figure 3: Block diagram of the main VI

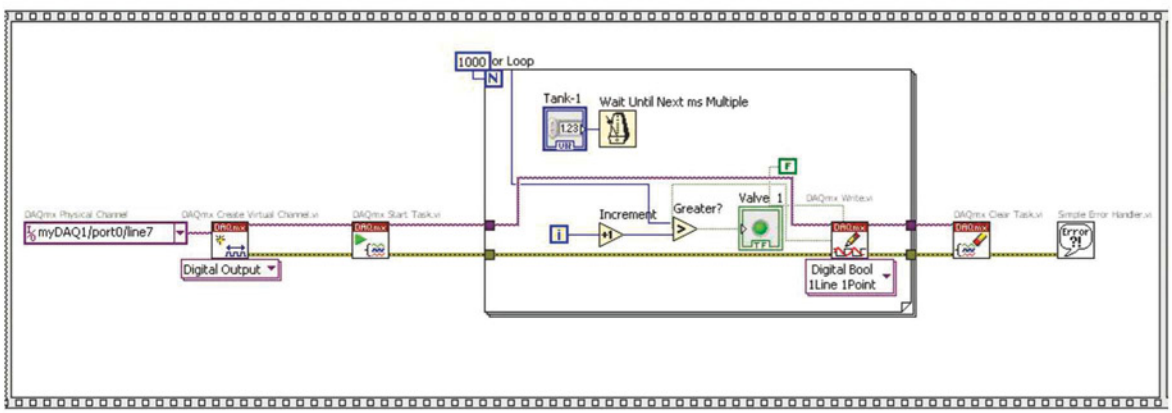

Figure 4: Section of the main VI which operates Valve 1

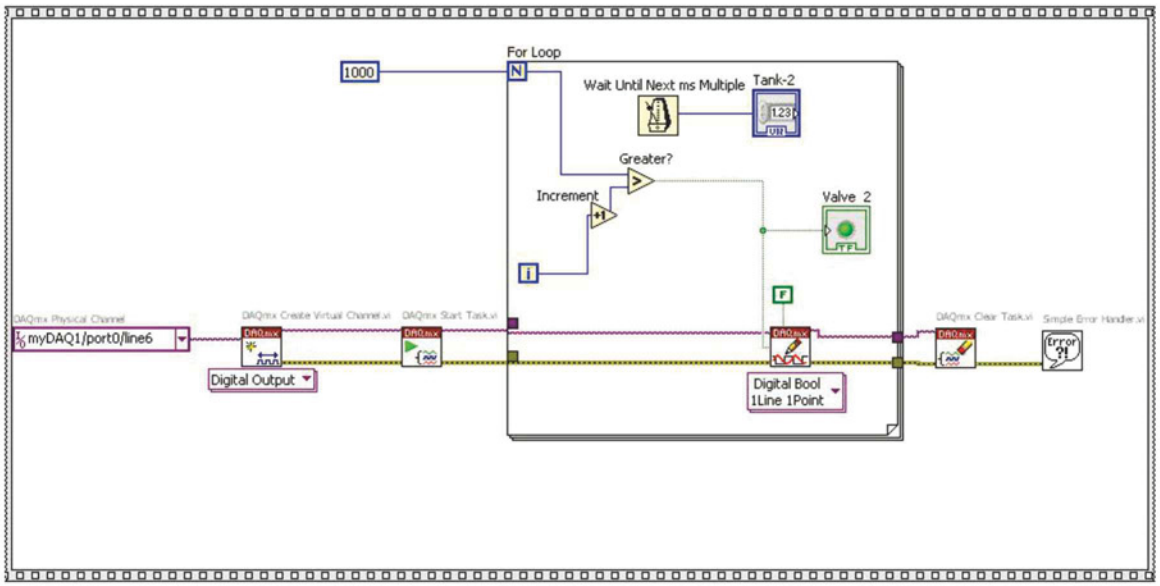

Figure 5: Small section of the main VI that operates Valve 2

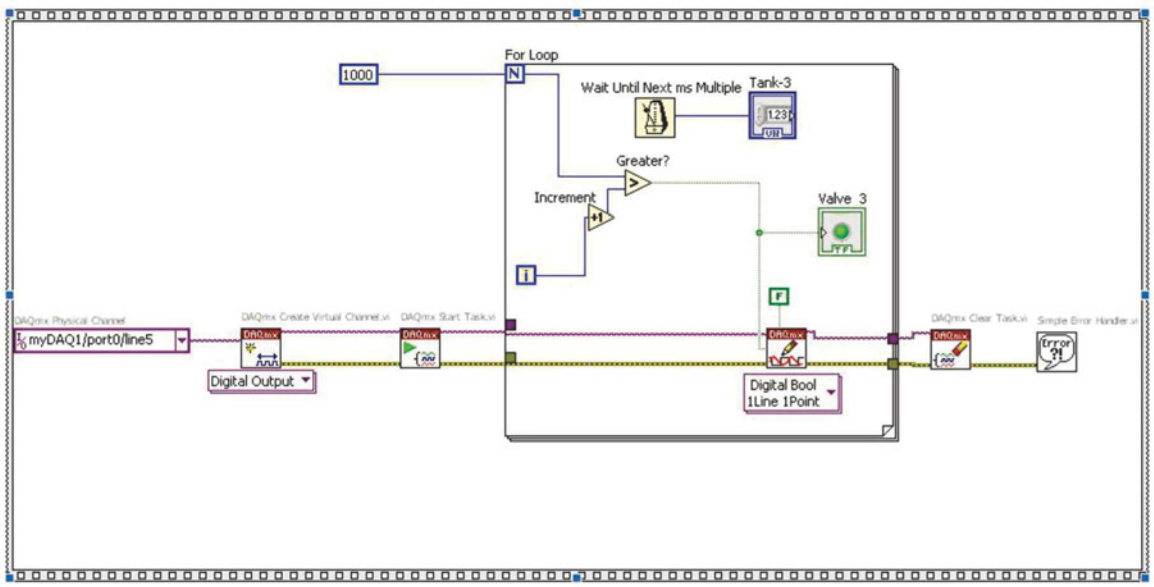

Figure 6: Section of the main VI that operates Valve 3

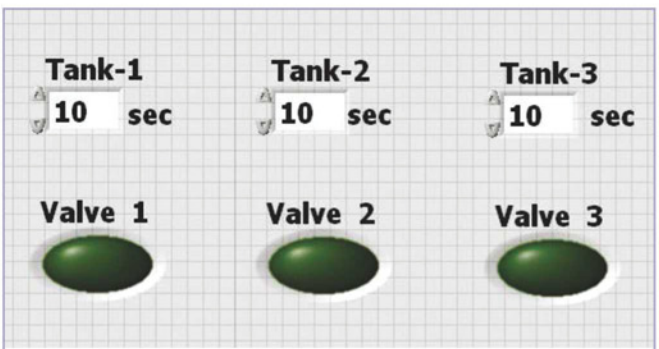

Figure 7: VI's front panel

VI's Front Panel

On the front panel Tank 1, 2 and 3 are controls and Valve 1, 2 and 3 are indicators. Valve operation timing can be set easily using the Tank 1, 2 and 3 fields. For instance, in Figure 7, Tank 1, 2 and 3 are set to 10s, which means that valve 1 will turn ON for 10s, letting in the chemical from tank 1. After 10s, the process repeats for valve 2, and then valve 3.

The number of valves and the timings can be controlled easily by a single user, making this system very useful. The requirements for scalability and flexibility are also met.

In some applications, valves are operated according to temperature, a modification done easily by adding temperature sensors. ●

www.electronicsworld.co.uk

Electronics WORLD

T&M supplement

TELEDYNE LECROY
Everywhereyoulook™

Teledyne LeCroy's 8 Channel Oscilloscopes

12-bit Accuracy up to 1 GHz

HIGH-DEFINITION OSCILLOSCOPES: SIGNAL ANALYSIS WITH 16-BIT VERTICAL RESOLUTION

BY SYLVIA REITZ, PRODUCT MANAGER FOR OSCILLOSCOPES AT ROHDE & SCHWARZ IN MUNICH

For oscilloscopes, vertical resolution is increasingly considered a key parameter, alongside bandwidth, sampling rate and memory depth. This development is driven by the heightened demand for greater signal detail in applications such as consumer electronics, medicine and R&D. The particular challenge is to measure low-voltage components with granularity of only a few hundred mV on a signal that also has high-voltage components.

INCREASING VERTICAL RESOLUTION WITH FILTER GAIN

The vertical resolution of an oscilloscope determines how accurately signals are displayed, and is responsible for the precision of the achieved measurement results. Just a few years ago a typical oscilloscope had a vertical resolution of 8 bits. However, when the signal under test has a high dynamic range (with low- and high-voltage components), 8-bit resolution may not be precise enough to meet the measurement requirements. This is why high-definition oscilloscopes with higher vertical resolution have come to market.

One option for increasing vertical resolution is with higher-resolution A/D converters. However, higher-resolution converters tend to have non-ideal properties such as offset, linearity and quantization errors that substantially decrease the overall effective number of bits (ENOB).

Another option is to use digital post-processing algorithms which increase resolution to a maximum of 16 bits – a 256-fold

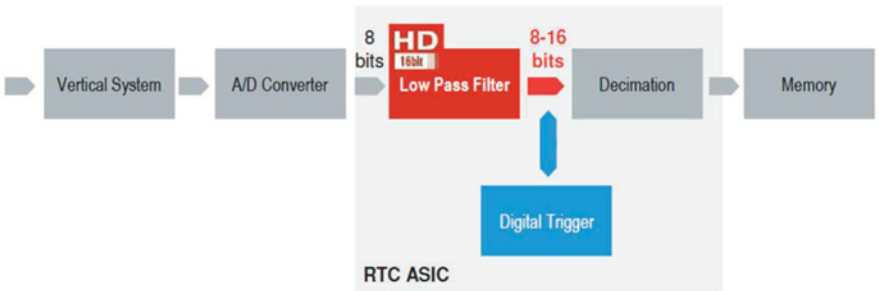

Figure 1: In R&S RTO and RTE oscilloscopes, the low-pass filter is positioned directly after the A/D converter, increasing vertical resolution

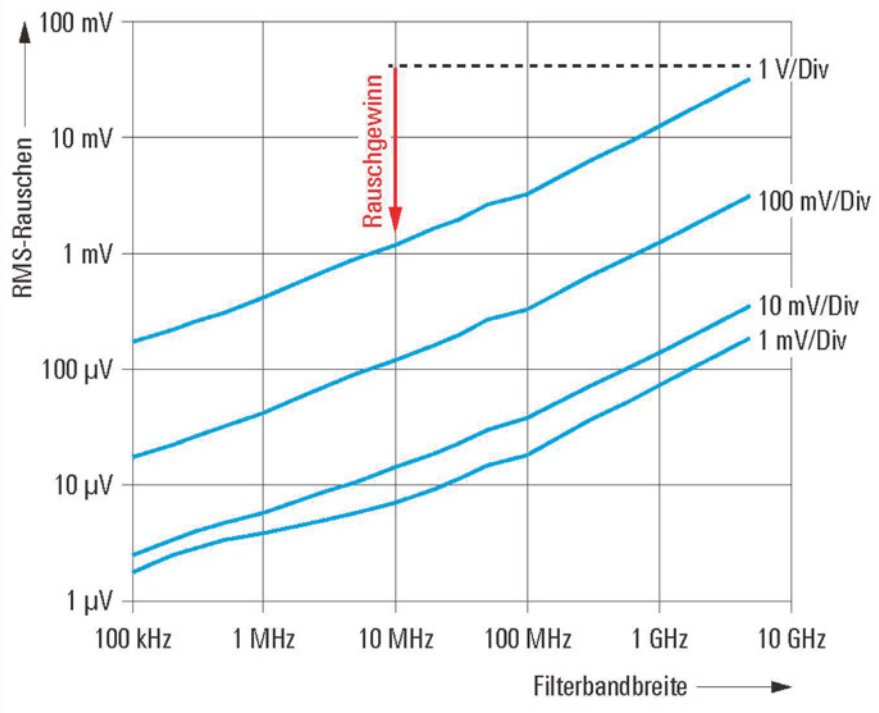

Figure 2: Noise of the R&S RTO1044 oscilloscope (4GHz model) as a function of the filter bandwidth set to high-definition mode. A reduction in noise leads to higher SNR, improving resolution

From 50 MHz to 4 GHz: Powerful oscilloscopes from the T&M expert.

FROST & SULLIVAN 2015 BEST PRACTICES AWARD
Global Oscilloscopes Competitive Strategy Innovation and Leadership Award

Visit us at **productronia** in Munich, hall A1, booth 375

Fast operation, easy to use, precise measurements –
That's Rohde & Schwarz oscilloscopes.

R&S®RTO: Analyze faster. See more. (Bandwidths: 600 MHz to 4 GHz)
R&S®RTE: Easy. Powerful. (Bandwidths: 200 MHz to 2 GHz)
R&S®RTM: Turn on. Measure. (Bandwidths: 200 MHz to 1 GHz)
R&S®HMO3000: Your everyday scope. (Bandwidths: 300 MHz to 500 MHz)
R&S®HMO Compact: Great Value. (Bandwidths: 70 MHz to 200 MHz)
R&S®HMO 1002: Great Value. (Bandwidths: 50 MHz to 100 MHz)

All Rohde & Schwarz oscilloscopes incorporate time domain, logic, protocol and frequency analysis in a single device.

Take the dive at www.scope-of-the-art.com/ad/all

HD 16bit

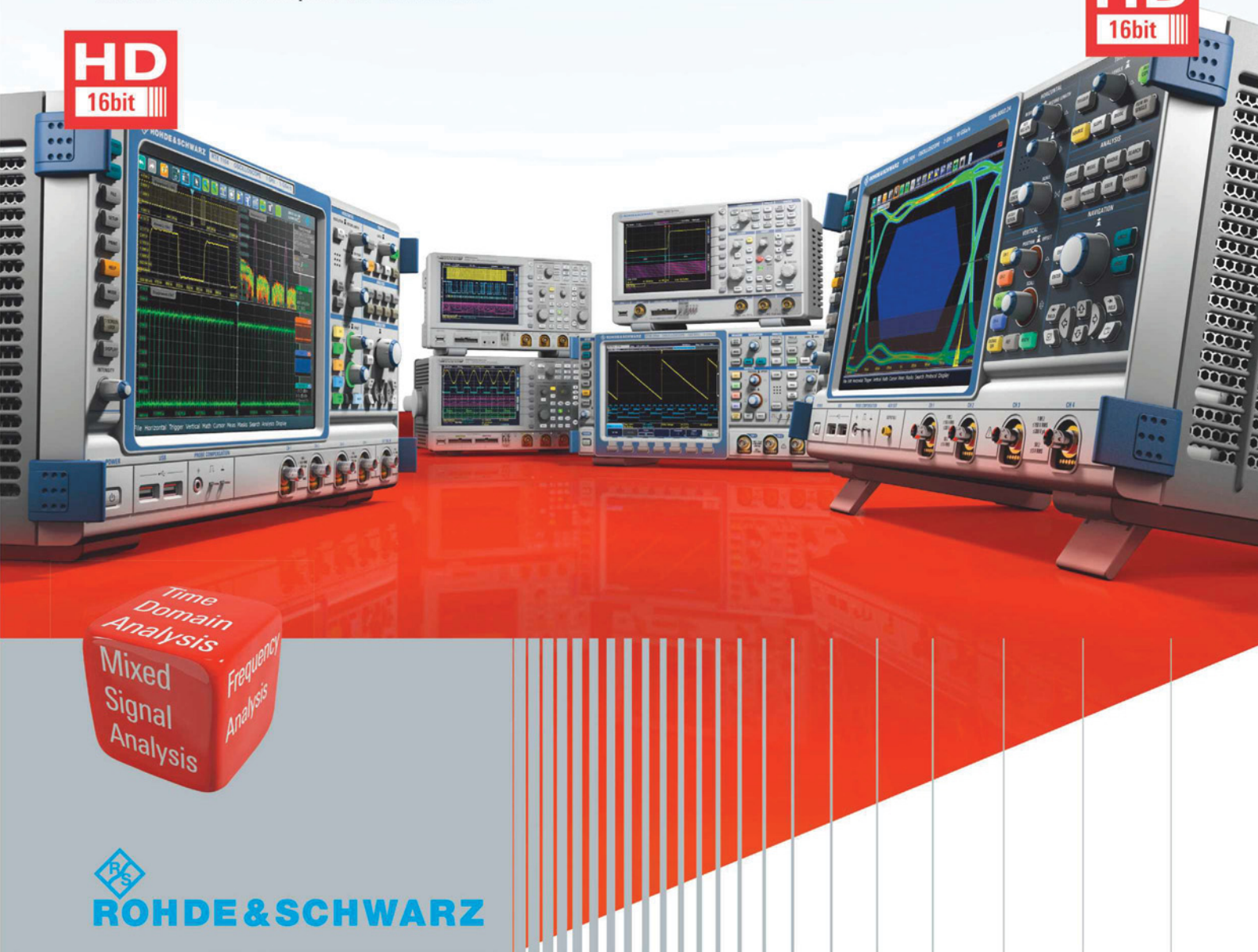

ROHDE&SCHWARZ

improvement over 8-bit resolution in standard mode. For example, the R&S RTO-K17 and RTE-K17 high-definition oscilloscopes use a digital low-pass filter implemented directly after the A/D converter in the oscilloscope's ASIC (Figure 1). The filter reduces noise, thereby increasing the signal-to-noise ratio (SNR) and vertical resolution. Users can adjust the bandwidth of the low-pass filter from 10kHz to 1GHz as needed, to match the characteristics of the applied signal.

The associated filter bandwidth determines the nominal resolution (Table 1). The lower the filter bandwidth as compared to the instrument bandwidth, the higher the resolution and noise reduction (Figure 2). This is illustrated by the spectrum shown in Figure 3, where f_a is the sampling rate of the oscilloscope, f_B is the bandwidth of the low-pass filter and S(f) is the signal. Assuming pure white noise (AWGN), which is a good approximation for a high-quality A/D converter, and assuming an ideal low-pass filter, the gain in the SNR is:

SNRgain = 10log(f_a/2f_B).

Filter	Vertical resolution
inactive	8 bit
1GHz	10 bit
500MHz	12 bit
300MHz	12 bit
200MHz	13 bit
100MHz	14 bit
50MHz to 10kHz	16 bit

Table 1: Vertical resolution of the R&S RTO oscilloscope as a function of the selected filter bandwidth in high-definition mode

SIGNAL DETAIL AND ACCURACY

Increase in resolution leads to sharper waveforms, showing signal details that would otherwise be masked by noise. Increasing input sensitivity to 500µV/div allows detailed analysis of these small signals, and thanks to the low-noise front-end and the highly accurate single-core A/D converter, these oscilloscopes have excellent dynamic range and measurement accuracy. Switching on high-definition mode allows users to benefit from even more precise measurement results, as seen in Figures 4 and 5.

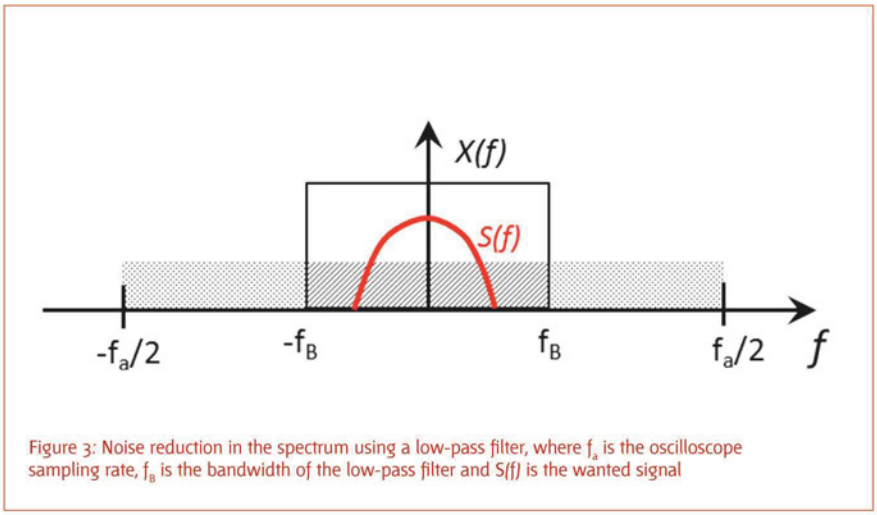

Figure 3: Noise reduction in the spectrum using a low-pass filter, where f_a is the oscilloscope sampling rate, f_B is the bandwidth of the low-pass filter and S(f) is the wanted signal

The ability to trigger on the smallest signal details so they can be reliably displayed depends strongly on the capabilities of the trigger system, such as its sensitivity. Each sample up to 16-bit is checked against the trigger condition and can initiate a trigger (see Figures 1 and 6).

In contrast, a traditional analogue trigger system cannot trigger on the high-resolution signal details because they are masked in the trigger path by the hysteresis of the analogue components.

> *"For oscilloscopes, vertical resolution is increasingly considered a key parameter, alongside bandwidth, sampling rate and memory depth"*

HIGH-DEFINITION MODE VS HI-RES DECIMATION

Oscilloscopes with a high-definition option offer significant advantages over the high-resolution (Hi-Res) decimation mode (used by most oscilloscopes on the market). First, the user knows exactly what signal bandwidth is available due to explicit low-pass filtering; second, there are no unexpected aliasing effects.

High-definition mode is not based on decimation, meaning that even in high-definition mode R&S RTO oscilloscopes still maintain a sampling rate of 5Gsample/s (or 2.5Gsample/s for R&S RTE oscilloscopes), ensuring the best possible time resolution.

High acquisition rate and functional range for fast measurement results ensures minimum compromise on measurement speed and options. Since the low-pass filtering is in real time, acquisition and processing rates remain high, also guaranteeing smooth operation of the oscilloscope.

All analysis tools, including automatic measurements, FFT and history mode, remain available in high-definition mode.

EXAMPLE: MEASURING RDS(ON) OF A DC/DC CONVERTER

Switched-mode power supplies are an integral part of modern electronic devices. They transfer power from source to drain and at the same time convert the current and voltage so the correct power is supplied to the components.

One criterion for classification of switched-mode power supplies is the type of input or output voltage. For example, a DC/DC converter converts one DC voltage at the input into a different DC voltage with either higher (up-converter) or lower (down-converter) voltage level.

There are many applications for DC/DC converters, ranging from PC or laptop power supplies to mobile phones and automobiles. Because of their switching speed, metal oxide semiconductor field effect transistors (MOSFETs) are typically used as switches,

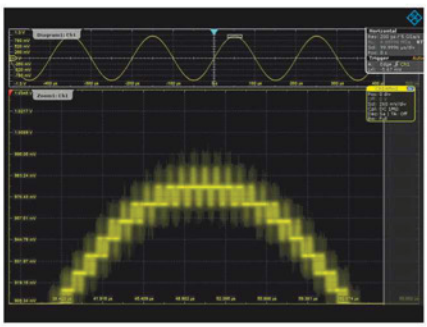

Figure 4: Zoomed-in peak of a sine wave. High-definition mode is not activated. Only the quantization levels can be seen in the zoom window

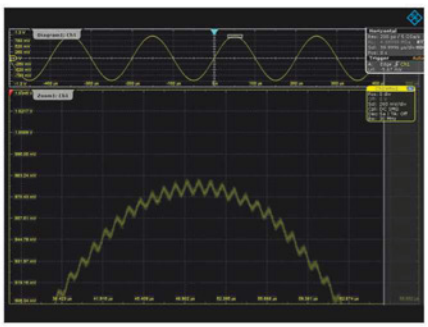

Figure 5: When high-definition mode is switched on, the zoom window shows that another, very low-amplitude, sine wave is superimposed on the signal

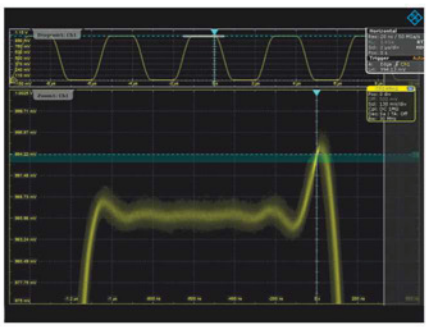

Figure 6: The high sensitivity of the digital trigger makes it possible to trigger on signal overshoots of less than 9mV, as can be seen in this example. At a vertical scale of 130mV/div, this corresponds to only a fraction of one display division

Figure 7: Measurement of the drain-source voltage of a DC/DC converter without high-definition mode. The large noise component in the signal makes reliable results impossible

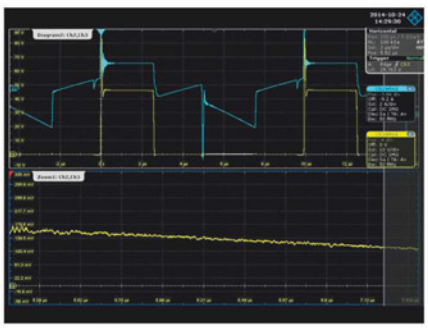

Figure 8: Measurement of the drain-source voltage of a DC/DC converter with high-definition mode. Increasing the vertical resolution to 16 bits makes the signal details visible

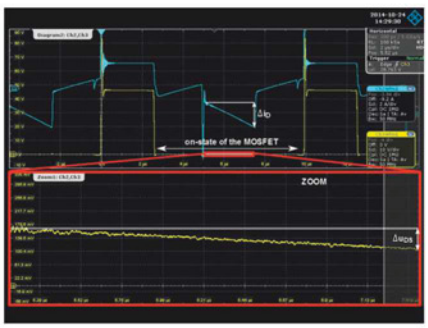

Figure 9: $R_{DS(on)}$ is calculated differentially from Δu_{DS} and Δi_D

although the efficiency of the transistor is clearly a key factor.

The power loss must be as low as possible, regardless of type. A key parameter in this respect is $R_{DS(on)}$. When switched on, the transistor acts as a resistor between the drain and the source. The value of this resistance, which differs depending on the operating point, determines the power loss of the converter.

$R_{DS(on)}$ of a DC/DC converter is calculated from the drain current and the drain-source voltage. Both must therefore be measured accurately.

Measurement of the drain-source voltage is particularly challenging with an oscilloscope. When the transistor is switched on, the voltages are very low, in the range of a few hundred mV. Conversely, very high voltages are present when the transistor is switched off. In extreme cases, the voltage variation between the transistor being switched on and off is several hundred volts. As seen in Figures 7 and 8, resolution of more than 8 bits is necessary for precise measurement of the low voltages.

The top half of Figure 7 shows the complete switching cycle of a MOSFET transistor, while the lower half shows a zoomed view of the drain-source voltage being measured. The waveforms were recorded with 8-bit vertical resolution. The noise component of the signal is too large to permit reliable measurement of the drain-source voltage. On the other hand, switching on high-definition mode and using a vertical resolution of 16 bits reduces the noise significantly, providing sharper waveforms and showing more details (Figure 8). This ensures precise measurement results and makes it possible to calculate the converter's $R_{DS(on)}$.

For completeness, it must be pointed out that a Rogowski coil was used to measure the drain current in this example. Rogowski coils capture only the AC components in the signal, which means that the current waveform on the oscilloscope display must include a DC offset. Therefore, to obtain an accurate result for $R_{DS(on)}$, it is not sufficient to simply divide an individual voltage value by the associated current value; a differential approach must be used instead. While the transistor is switched on, both the drain-source voltage and the drain current increase almost continuously within a defined time period. As seen in Figure 9, $R_{DS(on)}$ is therefore calculated based on Δu_{DS} and Δi_D within this time period. ■

HDO8000

8 Channel, True 12-bit Oscilloscopes with up to 1 GHz Bandwidth

HDO8000 High Definition Oscilloscopes provide more channels, more resolution, more bandwidth and more memory. They are ideal for debugging three-phase power electronics, automotive electronics, and mechatronic systems. Mixed Signal capability allows users to simultaneously analyze 8 Analog inputs and 16 Digital inputs. Serial data Trigger, Decode, and Analysis toolsets aid in debugging embedded systems. The unique Q-Scape multi-tab display makes it easy to work with multiple channels, and the solution is completed by a wide variety of probes and application packages.

Additionally, complex embedded and mechatronic designs used in automotive and consumer products contain a huge number of analog, digital, power, serial data and sensor signals that makes debug challenging and time-consuming. New instrument paradigms – more channels with higher resolutions at high bandwidths – are needed to meet these expanding and emerging needs.

Teledyne LeCroy has this new instrument – the HDO8000 Series, an 8 channel, 12-bit resolution, 1 GHz mixed-signal oscilloscope with the most comprehensive serial data, probe and application package toolsets. Use the HDO8000 to examine power electronics device or three-phase output signals, high-speed microprocessor signals, or analog, digital or serial data traffic on an embedded control board. Now, you have enough to do it all.

HIGH-POWER, THREE-PHASE POWER ELECTRONICS

Variable frequency motor drive designs are increasingly down-deployed in lower cost applications, but with increasing control complexity. Distributed electric power generation is increasing the demand for inverters and converters to interface these power sources to the grid, and is also driving new power electronics solutions to compensate, regulate and control the power flow from large amounts of distributed generation.

With the HDO8000, it is possible to monitor three-phase voltages and currents simultaneously along with the DC bus or other control and sensor signals. Use serial/logic triggers to isolate/correlate control or external events to establish cause and effect. 12-bit resolution provides capability for full power section characterization from device switching and conduction losses to output measurements. 1 GHz bandwidth measures the fast rise times and switching speeds of SiC and GaN devices, and also permits embedded control debug on today's fastest 32-bit microprocessors. 250 Mpts/ch of memory permits the most comprehensive analysis of mixed low-speed and high-speed events over long periods of time.

AUTOMOTIVE ELECTRONICS, HYBRID/ ELECTRIC VEHICLE PROPULSION

Hybrid electric and electric vehicles (HEVs and EVs) use high-power DC-DC converters for two-way conversion of power between propulsion systems and other loads and the high voltage, 48V, and 12V distributed DC buses/batteries. Automotive electronic control units (ECUs) are tested to some of the most stringent standards – more channels provides more insight faster. 12-bits and 250 Mpts provides the amplitude and time resolution needed for better and more intuitive cause effect analysis. Deep digital logic, trigger, decode and analytic toolsets provides an all-in-one characterization tool for the complex, dynamic behavior of the vehicle ECUs.

EMBEDDED, MECHATRONIC SYSTEMS

Today's consumer appliances and industrial systems combine complex embedded controls, power electronics, and sensors to achieve the highest efficiency and provide important benefits. Time-to-market, cost and quality pressures place exceptional demands on new product test, debug and troubleshooting. HDO8000 capabilities provide more insight faster.

HIGH-PERFORMANCE 16-CHANNEL MIXED SIGNAL CAPABILITY

With embedded systems growing more complex, powerful mixed signal debug capabilities are an essential part of modern oscilloscopes. The 16 integrated digital channels and set of tools designed to view, measureand analyze analog and digital signals enable fast debugging of mixed signal designs.

TRUE 12-BIT HARDWARE

Teledyne LeCroy HDO high definition oscilloscopes use unique HD4096 technology to provide superior and uncompromised measurement performance: 12-bit ADCs with high sample rates, High signal-to-noise amplifiers (55 dB), and Low noise system architecture up to 1 GHz

Oscilloscopes with HD4096 technology have higher resolution than conventional 8-bit oscilloscopes (4096 vs. 256 vertical levels) and low noise for uncompromised measurement performance. The 2.5 GS/s, 12-bit ADCs support capture of fast signals and oscilloscope b<andwidth ratings up to 1 GHz. The high performance input amplifiers deliver pristine signal fidelity with a 55 dB signal-to-noise ratio. The low-noise system architecture provides an ideal signal path to ensure that signal details are delivered accurately to the oscilloscope display – 16x closer to perfect.

Image 1 - Monitor three-phase voltages and currents simultaneously along with the DC bus or other control and sensor signals

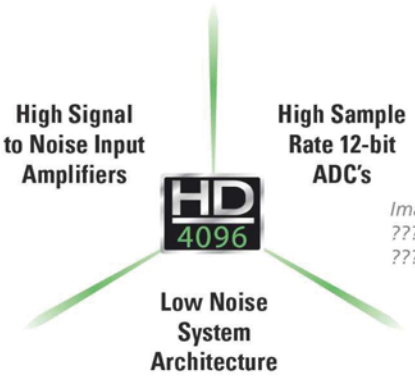

Image 2 - ????? ??????? ?????? ?????

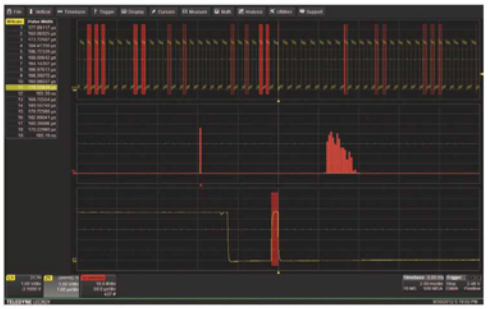

Image 3 - WaveScan allows searching analog, digital or parallel bus signal in a single acquisition using more than 20 different criteria.

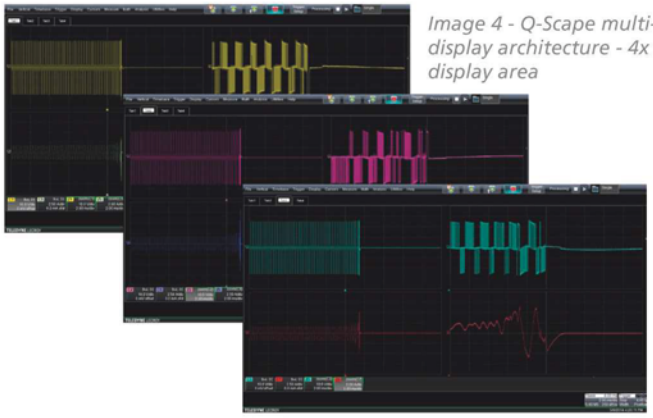

Image 4 - Q-Scape multi-tab display architecture - 4x the display area

EXTENSIVE TRIGGERING

Flexible analog and digital cross-pattern triggering across all 20 channels provides the ability to quickly identify and isolate problems in an embedded system. Event triggering can be configured to arm on an analog signal and trigger on a digital pattern.

TRIGGER AND DECODE

The serial data trigger will quickly isolate events on a bus eliminating the need to set manual triggers and hoping to catch the right information. Trigger conditions can be entered in binar y or hexadecimal formats and conditional trigger capabilities even allow triggering on a range of different events. Protocol decoding is shown directly on the waveform with an intuitive, color-coded overlay and presented in binary, hex or ASCII. Decoding on the HDO8000 is fast even with long memory and zooming in to the waveform shows precise byte by byte decoding.

Supported Serial Data Protocols:

- I2C, SPI, UART
- CAN, LIN, FlexRay™, SENT
- Ethernet 10/100BaseT, USB 1.0/1.1/2.0, USB 2.0-HSIC
- Audio (I2S, LJ, RJ, TDM)
- MIL-STD-1553, ARINC 429
- MIPI D-PHY, DigRF 3G, DigRFv4
- Manchester, NRZ

WAVESCAN ADVANCED SEARCH

WaveScan provides powerful isolation capabilities that hardware triggers can't provide. WaveScan allows searching analog, digital or parallel bus signal in a single acquisition using more than 20 different criteria. Or, set up a scan condition and scan for an event over hours or even days.

Since the scanning "modes" are not simply copies of the hardware triggers, the utility and capability is much higher. For instance, there is no "frequency" trigger in any oscilloscope, yet WaveScan allows for "frequency" to be quickly "scanned." This allows the user to accumulate a data set of unusual events that are separated by hours or days, enabling faster debugging. When used in multiple acquisitions, WaveScan builds on the traditional Teledyne LeCroy strength of fast processing of data. Quickly scan millions of events looking for unusual occurrences, and do it much faster and more efficiently than other oscilloscopes can. Found events can be overlaid with the ScanOverlay to provide a quick comparison of events; measurement based scans populate the ScanHistogram to show the statistical distribution of the events. Using the powerful parallel pattern search capability of WaveScan, patterns across many digital lines can be isolated and analyzed. Identified patterns are presented in a table with timestamp information and enables quick searching for each pattern occurrence.

Q-SCAPE MULTI-TAB DISPLAY ARCHITECTURE

Q-Scape tabbed displays quadruples the display area and provide faster insight. Acquired or calculated waveforms can be located on any of four different "tabbed" oscilloscope grid displays, with individually selectable grid styles available for each tab. Q-Scape is ideal for three-phase analysis with many analog and digital acquired and calculated waveforms.

LABNOTEBOOK

The LabNotebook feature of HDO8000 provides a report generation tool to save and document all your work. Saving all displayed waveforms, relevant settings, and screen images is all done through LabNotebook, eliminating the need to navigate multiple menus to save all these files independently. ■

teledynelecroy.com

BUYING USED WITHOUT RISK

BY GEORGE ACRIS, SALES AND MARKETING DIRECTOR AT MICROLEASE

Technology companies need to maintain a fleet of calibrated, serviceable instruments, ready for use by their engineers. This represents a serious investment. Whilst most engineers and buyers are comfortable with buying or leasing new equipment where a requirement is long term, and renting where equipment is needed for a specific project only, there can be more concern when considering the used-instrument market.

Recognising an opportunity, there is a growing trend for leading rental companies to offer quality-guaranteed used instruments. Buying used need no longer mean taking a flyer on an instrument of unknown provenance from an obscure source. It can be a genuine and cost-effective alternative. And the used market provides the opportunity to realize a financial return on instruments that are no longer needed.

QUALITY CHECKS AND CALIBRATION

The great advantage of sourcing used equipment from a well-known rental company is that they will not want to associate their name with a sub-standard instrument.

Reputable companies put the equipment through a rigorous certification programme before allowing it to be resold. These programmes will include electrical and functional tests, validation and full refurbishment. Firmware and other software will be updated, a full internal and external cleaning carried out, and cosmetic issues rectified, such as damaged controls and feet. In most cases the instrument will be calibrated to ensure it operates to manufacturer specifications. The quality will be reflected in the price, but that old adage "you get what you pay for" is certainly true in this case.

> *"The used market provides the opportunity to realize a financial return on instruments that are no longer needed"*

Prior to shipment, the instrument is configured to order. This includes configuring the user interface language and time zone setting for the destination country. Instruments are supplied with all the standard accessories originally included by the manufacturer, including any leads, manuals and disks, as well as the correct power lead for the destination country where applicable.

The service and support associated with these programmes is also similar to that for a new sale. The reseller will offer applications engineering support, to verify that the proposed instrument actually addresses the need. It may well be possible to add options if required, and the customer may be able to negotiate the removal of those they don't need to bring down the cost. Many features are now delivered in software, allowing an approved reseller to easily adjust the specification.

Some suppliers offer warranties that guarantee their certified pre-owned instruments are not only serviceable but also fit for the customer's intended purpose, with rights of return if dissatisfied. Some suppliers offer ongoing technical support, particularly valuable if you are unfamiliar with the equipment.

EXPLORING THE OPTIONS

Of course, a conversation with a rental company can look more widely at the challenge the customer faces and explore other alternatives. Test equipment is getting more sophisticated. This means it is generally getting more expensive and at the same time becoming obsolete more quickly. Couple this with the fact that companies are increasingly looking to get as many assets as possible off their balance sheets, and the alternatives to owning start to look quite attractive. Depending on the timeframe over which the equipment is to be used, rental or operating leases should be investigated before deciding the best option.

Very often rental may turn out to be a better solution than taking on the obligations of outright ownership of an instrument, considering the costs of servicing, calibration and other maintenance, and the usage time of the equipment. Rent-to-buy suits companies that need the test equipment immediately but do not have the budget available or have to wait for a sign-off that may take months.

Different leasing methods are also available:

Figure 1: Instruments stand ready for shipment at the Microlease Harrow (UK) headquarters

finance leases, operating leases and operating leases with services. These enable companies only to pay for the equipment while they need it with no upfront costs, and the flexibility to upgrade the equipment in the future.

PART-EXCHANGE

Programmes like the Certified Pre-Owned from Microlease offer customers quality surplus equipment with a potentially effort-free financial return. There probably isn't a single company that doesn't own a piece of test equipment that it no longer uses. Most resellers of test equipment also buy it. Customers can trade in assets sitting in a cupboard somewhere and reduce purchase cost. They could even end up with a credit! If the supplier offers trade-ins, customers may also be able to trade up in the future the equipment they are buying now. This may be an important consideration.

An assessment of specification and condition is done promptly, after which the equipment can be accepted for part-exchange or for a cash sum, and go through an intense 23-point refurbishment process.

Managing a test instrument fleet and making the right decisions on when to buy, what to buy, when to rent and when to sell is difficult. For this reason, customers are entering into strategic partnerships that make use of rental companies' expertise in asset management. This service can include a simple audit, compiling a clean database of inventory, including information that that allows you to make decisions and helps with location changes, condition, usage, calibration status and disposal of surplus equipment.

USED: A REAL ALTERNATIVE

Instruments sourced from a manufacturer's recognised program or a reputable source can provide a genuine alternative to buying a new instrument at a significant saving; purchasing managers can and should investigate this as part of their requisition process. Using a reputable source with a good warranty, backed by a stringent certification program, mitigates much of the risk associated with purchasing a used instrument. ■

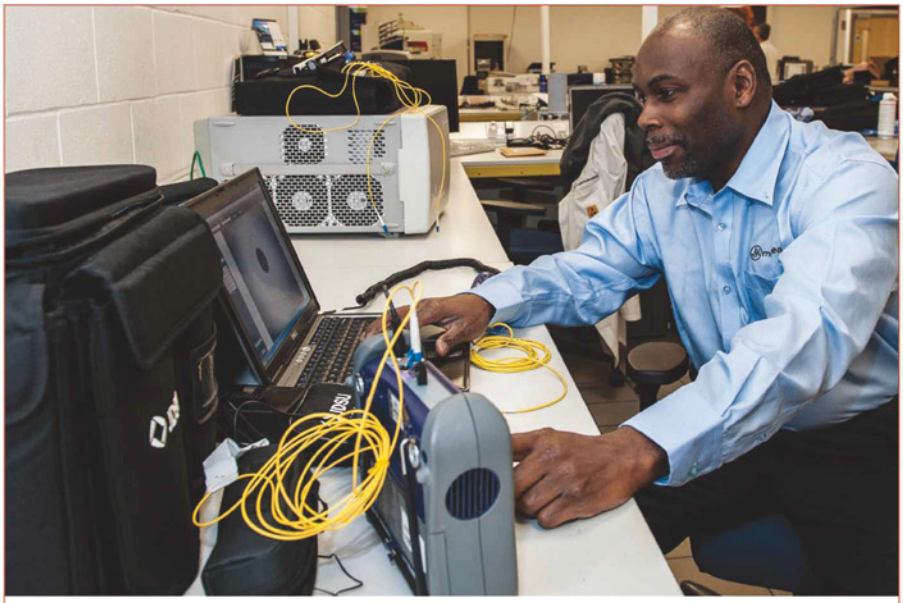

Figure 2: An instrument being checked and calibrated before shipment by a Microlease technician

Figure 3: Rental companies like Microlease carry a huge range of equipment from many different manufacturers

Figure 4: It is essential that instruments are stored in controlled conditions when not in use. These are the specially designed Kardex storage units at Microlease headquarters in Harrow

LINK MICROTEK RECREATES HIGH-POWER AVIONICS TEST SYSTEM

Link Microtek has recreated an obsolete test system for a prime contractor in the defence industry to enable the end customer to continue critical support for an avionics EW (electronic warfare) system.

With its expertise in microwave engineering, electronics and mechanical design, Link Microtek was able to reproduce the complex unit working only from a set of old drawings and some parts. The unit was originally designed over 25 years ago, and no other specifications or technical details were available.

"As is often the case when dealing with obsolescence, most of the original assembly instructions and knowledge had been lost in the mists of time," commented Steve Cranstone, Link Microtek's managing director. "So that did make it a challenging project, not least in recreating the exact same full-custom end-plate castings, which form the precision interface with the avionics system."

www.linkmicrotekeng.com

NEW EYEPIECE-LESS STEREO MICROSCOPE AIDS PRODUCTIVITY

Vision Engineering launched Lynx EVO, a new high productivity eyepiece-less stereo microscope, ideal for inspecting PCBs, wafers, connectors, SMT products.

Lynx EVO eliminates the difficulty and strains of using 'eyepiece' stereo microscopes, opening up a world of enhanced productivity and ease of use.

Although the eyepiece-less advantage of Lynx EVO stems from stunning 3D (stereo) imaging, the real brilliance of the patented design is the simplicity of operation.

Superior imaging combined with unrivalled ergonomics promotes simple hand-eye co-ordination, critical for precision inspection tasks, re-work, repair and other manipulation activities. Operators can maintain the highest levels of performance, even across an entire shift.

Benefitting from a high optical specification, the 10:1 zoom ratio with long working distances provides users the ability to inspect up to 120x magnification (6-60x standard), ideal for a wide range of applications.

www.visioneng.com

RENEWED BALANCE PORTFOLIO FROM METTLER TOLEDO

After the successful market introduction of the MS-TS and ML-T balances, Mettler Toledo is pleased to complete the renewal of its portfolio with the launch of entry level balance, the ME-T. Designed to meet all essential needs, it offers a reliable, high-performance weighing cell and a large, intuitive 4.5" colour TFT screen, as well as three interface connections for easy data handling. It is the perfect choice for day-to-day weighing in any lab or manufacturing environment where value for money has high priority.

Built-in applications and an intuitive user interface make the ME-T convenient and easy to use, even for untrained operators. The weighing-in guide and large colour touchscreen with red and blue digits help users to dose to target and clearly indicate if sample weights are over or under tolerances.

www.mt.com

TBA SPRINGS TO ATTENUATION

Designed to keep out or keep in electromagnetic interference, TBA Protective Solutions range of BeCu gaskets are an excellent choice for shielding electronic equipment.

With attenuation exceeding 100dB for most profiles, the mechanical and electrical properties makes this high performance metal alloy ideal for EMI/RFI shielding, providing shielding effectiveness over an extremely broad frequency range giving a high deflection range and long life without compression set. BeCu gaskets give maximum spring properties for strength and fatigue resistance.

DiamondBack shielding, with a textured contact surface, increases attenuation at 2.5GHz and above. The non-abrasive texturing can be applied to most standard profiles to achieve up to 20dB attenuation improvement at high frequencies without raising the compression force.

To avoid galvanic action between contacting metals a variety of plating options are available.

www.tbaps.com

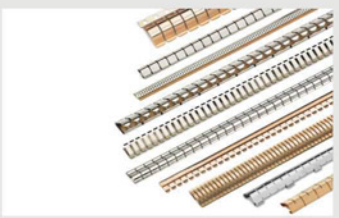

RENESAS SYNERGY EMBEDDED HARDWARE/SOFTWARE PLATFORM FIRST PRODUCTS

Renesas Electronics announced its first products in the company's new Synergy Platform, a qualified, easy-to-use environment designed to accelerate time to market, reduce total cost of ownership and remove many of the obstacles engineers face when designing Internet of Things (IoT) and other embedded applications. The platform's first products include the scalable S7G2 and S3A7 microcontroller (MCU) groups that target connected human-machine-interfaces (HMIs) and power-efficient control applications used in industrial, healthcare, home appliance and metering products. Development kits featuring the two MCU groups, software development tools and Renesas Synergy Software Package (SSP) are available now from the Renesas Synergy Gallery.

The Renesas Synergy Platform gives designers direct access to a completely integrated real-time operating system (RTOS) with communication stacks, middleware, libraries, an application framework and the MCUs' drivers and peripherals.

www.renesas.eu

NEW EMBEDDED CONTROLLERS FROM CAMBRIDGE MICROPROCESSOR SYSTEMS

Cambridge Microprocessor Systems has released its latest range of embedded controllers – PROton Embedded Systems. Currently with three ARM-based controllers in the range, these products are fast and extremely flexible to use.

PROton boards support a full range of interfaces including SPI, I2C, UART, CAN, USB and Ethernet. They also offer timers, counters, encryption, digital and analogue I/O. For further memory and peripheral expansion a range of plug in shields are available.

Development tools and real-time multi-tasking software for the PROton controllers are provided free of charge by download. For more details visit the website at www.proton-es.co.uk.

Cambridge Microprocessor Systems also offers bespoke hardware and software design services, offering low-cost, fast-turnaround, customised products to customer requirements.

www.cms.uk.com

HARWIN SECURES RELIABLE COAX CONNECTION IN CHALLENGING ENVIRONMENTS

Harwin launched a range of standard layout, multiport coaxial Datamate connectors with 6GHz, 50Ω contacts, suitable for hi-rel applications. Suitable for RG178 cables, the ganged connectors are available from stock with two, four, six or eight contacts.

Based on Harwin's proven high-reliability Datamate connector family, the new coax connectors are designed with a single body moulding to resist extremes of shock, vibration and temperature in challenging application environments such as defence, aerospace, satellites, UAVs, undersea and more.

Devices are equipped with hexagonal slotted jackscrews for secure fixing to the PCB, and mouldings are polarised to facilitate quick, error-free mating. Vertical and horizontal orientation styles are available, and Harwin offers a choice of products to suit 3.5 and 5mm PCB thicknesses.

www.harwin.co.uk

NEW LASER MARKING EQUIPMENT AT AWS ELECTRONICS

AWS Electronics Group is supporting significant growth in the automotive sector by investing in an inline laser marker. The company is currently already contracted to produce in excess of three million automotive PCBs in 2016, and this investment in high-end equipment from German manufacturer, Asys, is much more accurate and 30% faster than traditional automatic label marking previously used by the company. It also increases AWS's board marking capacity by 50%.

AWS has won several significant automotive programs recently, both at its UK Technical Centre in the UK and its low manufacturing cost facility in Namestovo Slovakia.

"The Asys laser marking machine has already proved its mettle – it has been running now for three months at upwards of 4000 units per day and has yet to produce a single bad mark," said AWS's Group Technical Director, Robert Lackey.

www.awselectronicsgroup.com

AWS ELECTRONICS GROUP

HIGH-OUTPUT, HIGH-EFFICIENCY OSRAM SFH 471XAS IREDS

Mouser Electronics is now stocking the new SFH 4715AS and SFH 4716AS infrared LEDs (IREDs), part of the IR OSLON Black family from OSRAM Opto Semiconductors. These small infrared LEDs improve on previous generations of OSLON Black SFH 471x IREDs, increasing output to over 1W.

The SFH 471xAS IREDs are built on an optimized package and Nanostack technology, in which each chip has two emission layers. Depending on the type of camera and number of infrared light emitting diodes, the SFH 471xAS can provide illumination over a distance of more than 328 feet (100m), which make them ideal IR light sources for many camera-based applications.

OSRAM OSLON Black SFH 4715AS and SFH 4716AS IREDs come in a small 3.85mm² package with an integrated lens that allows superior compact arrangements of very high power density.

To learn more about OSRAM IR OSLON Black SFH 471xAS, visit:

www.mouser.com

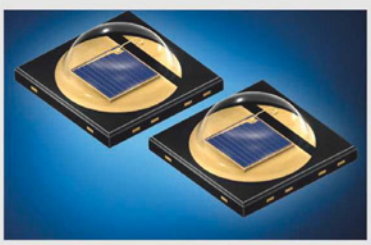

OMC OFFERS TO MOUNT ANY FIBRE OPTIC DIODE IN ANY HOUSING

OMC, optoelectronics manufacturer, has announced a new service, enabling engineers to choose exactly the right fibre optic diode for their application and have it mounted in their preferred package.

Although the company offers a wide standard range of packaged transmitters and receivers, it also recognises that sometimes designers have specific requirements which demand a custom approach. "We regularly get approached by people who have identified a diode which is a perfect match for their needs. As the housing itself – as well as the way the diode is mounted in the housing – can have serious implications for system performance, we decided to offer a 'mix and match' service, where you specify housing and diode, we'll look after the mounting process," said OMC's Commercial Director, William Heath.

www.omc-uk.com

NEW RANGE OF ANTI-SURGE RESISTORS FROM PANASONIC

Panasonic Automotive & Industrial Systems introduced a new range of anti-surge resistors benefiting from capacitive-coupled isolation for high-temperature and small size requirements. Featuring a 0402 case size and a rated power of 0.2W, new ERJ-PA2 series resistors offer space savings without compromising on rated power specifications. A high ESD voltage of 3.0kV provides very high circuit reliability. A TCR of 100ppm and a tolerance of down to ±0.5% result in very stable resistance and circuit operation.

Panasonic's ERJ-PA2 series components benefit have been designed for a wide operating temperature range of -55°C up to +155°C and are ideal for use in automotive/transportation applications, industrial electronics, as well as consumer electronics. The devices are fully RoHS/REACH compliant, making them very environmentally friendly.

http://eu.industrial.panasonic.com

SIBEAM INTRODUCES NEW 60GHZ WIRELESSHD MODULES

SiBeam, a Lattice Semiconductor company, launched new WirelessHD transmitter and receiver modules that operate over the 60GHz millimeter wave frequency band. Based on production-proven WirelessHD chipsets already shipping in consumer electronic devices, the modules deliver visually lossless 1080p video streams at up to 60 frames per second and are an ideal video cable replacement solution in medical or industrial operating environments where cables are safety hazards. The wireless modules also reduce the cost of ownership in clean-room environments as there are no video cables to maintain and sterilize.

SiBeam's WirelessHD MOD6320-T transmitter and MOD6321-R receiver modules connect to a host board and provide wireless video connectivity between an HDMI source and a display. Having attained various wireless regulatory approvals, the modules significantly reduce the complexity associated with wireless performance design, testing and compliance standards in wireless system design.

www.sibeam.com

YOKOGAWA FACILITY RECEIVES ISO17025 ACCREDITATION

Yokogawa's European Calibration Laboratory has become the world's first non-governmental facility to receive full ISO17025 accreditation for power measurements of up to 100kHz. This is in addition to its established capability for providing high-accuracy calibration at 50Hz, especially at very low power factors (down to 0.0001) and at high currents.

The growth in renewable energy markets and the need to optimise energy efficiency while complying with international standards has been driving the demand for certainty in power measurements, especially at low power factors. In addition, the inverters used in renewable energy systems are switching at higher speeds: a scenario that introduces harmonics at higher frequencies.

There is also demand for high-frequency power measurements on switch-mode power supplies, electronic lighting ballasts, soft starters in motor controls and frequency converters in traction applications.

tmi.yokogawa.com

SYNCHRONOUS BUCK REGULATOR ICS FOR USB CHARGING

The new A8652 and A8653 from Allegro MicroSystems Europe extend the company's portfolio of automotive regulator ICs by adding two devices targeted specifically at USB power applications.

The new devices are high output current synchronous buck regulator ICs that provide tight load regulation over a wiring harness without the need for remote sense lines. This remote load regulation is achieved with an integrated open-loop correction scheme that, given a known wiring harness resistance, adjusts the output voltage based on the measured load current and a user programmable gain, achieving ±2% accuracy at 500mV of correction.

The remote load regulation control includes a 115% regulated voltage clamp in conjunction with a dynamic overvoltage protection circuit using threshold changing with the correction voltage.

Each device includes a user-configurable load-side current limit.

www.allegromicro.com

UNIQUE RFID ANTENNA ADAPTABLE TO CUSTOMER APPLICATIONS

Harting has developed a unique type of RFID antenna, the Ha-VIS LOCFIELD antenna, which uses a coaxial travelling-wave concept to offer users a compact package with complete flexibility in the design of RF reading zones. Not only is the antenna adaptable to every customer application, it is also ideal for situations where space is at a premium.

Modern industrial RFID systems allow components and packages to be followed in real time, and offer a multitude of options for increasing process security and ensuring optimal transparency. However, there is generally very little space available around belt conveyors, and classical RFID antennas are limited in that they cannot map curved tracks: a factor that restricts the capability for customers to track and trace production history at every point in the process.

www.harting.co.uk

PROTEUS 8.3

ECAD to MCAD made easy

Data Exchange with STEP/IGES

AUTODESK. PTC

SOLIDWORKS

The Proteus Design Suite now includes full support for data exchange with Mechanical CAD packages via the STEP/IGES file formats. This allows you to better visualise your design and helps quickly solve fixtures, fittings and casement problems.

Import 3D STEP/IGES models for your parts and visualise inside the Proteus Design Suite. Export your completed board to Solidworks or other MCAD software.

Visit www.labcenter.com

Tel:+44 01756753440 E-Mail info@labcenter.com

Labcenter Electronics Ltd, 21 Hardy Grange, BD23 5AJ

Labcenter Electronics www.labcenter.com

uk.mouser.com

The Newest Products for Your Newest Designs®

The **widest selection** of the **newest products**.

Over **4 million** products from over **500 manufacturers.**

Authorised distributor of semiconductors
and electronic components for design engineers.

MOUSER ELECTRONICS